25/1152

NUREG/CR-1152
SAND 78-1879

Recommended Methods for Estimating Atmospheric Concentrations of Hazardous Vapors After Accidental Release Near Nuclear Reactor Sites

Prepared by J.R. Connell, H.W. Church

Sandia Laboratories

Prepared for
U. S. Nuclear Regulatory Commission

NEWARK PUBLIC LIBRARY

MAY 20 1980

U. S. GOVT.
DEPOSITORY 37

READEX FICHE

Y3.N 88:

NOTICE

This report was prepared as an account of work sponsored by an agency of the United States Government. Neither the United States Government nor any agency thereof, or any of their employees, makes any warranty, expressed or implied, or assumes any legal liability or responsibility for any third party's use, or the results of such use, of any information, apparatus product or process disclosed in this report, or represents that its use by such third party would not infringe privately owned rights.

Available from

GPO Sales Program
Division of Technical Information and Document Control
U. S. Nuclear Regulatory Commission
Washington, D. C. 20555

and

National Technical Information Service
Springfield, Virginia 22161

NUREG/CR-1152
SAND 78-1879
RE

RECOMMENDED METHODS FOR ESTIMATING ATMOSPHERIC CONCENTRATIONS OF HAZARDOUS VAPORS AFTER ACCIDENTAL RELEASE NEAR NUCLEAR REACTOR SITES

J. R. Connell*

H. W. Church

Date Published: April 1980

Environmental Research Division 4533
Sandia Laboratories
Albuquerque, NM 87185
Operated by
Sandia Corporation
for the
U.S. Department of Energy

Prepared for
Division of Site Safety and Environmental Analysis
Office of Nuclear Reactor Regulation
U.S. Nuclear Regulatory Commission
Washington, D.C. 20555

NRC Fin No. A1110

*Work performed as visiting faculty-staff, now at Battelle/Pacific Northwest Laboratories.

UNITED STATES
NUCLEAR REGULATORY COMMISSION
WASHINGTON, D. C. 20555

FOREWORD

This literature survey of atmospheric transport and dispersion characteristics of hazardous substances provides a basis for recommendations for input to the evaluation of postulated accidents in the vicinity of nuclear reactor sites. The study was requested by the NRC staff to review the state-of-the-art with respect to the unique characteristics of some hazardous substances. Of the various components of this unique diffusion problem, the treatment of buoyancy (negative, neutral, or positive) characteristics was of paramount concern. In providing recommendations for interim guidance, this review clearly demonstrates the need for additional research and refinement. Work was substantially completed in 1978; therefore recent information may not be reflected in the review, but does not detract from an initial attempt to consolidate the elements of the problem.

Earl H. Markee, Jr., Leader
Meteorology Section
Hydrology-Meteorology Branch
Division of Site Safety and
Environmental Analysis

ABSTRACT

A literature survey was done which addresses the problems of atmospheric transport and diffusion of positively and negatively buoyant hazardous gases. Typical hazardous vapors of concern are chlorine, ammonia, and vapors from liquified natural gas. The objective was to determine the state of the art for analyzing hazards to nuclear power plants. It was found that existing computer simulations, and fluid laboratory and field measurements provide a basis from which to analyze the problem, but are insufficient for the establishment of firm hazards criteria. Within this report, existing models with predictive capability have been categorized, and available measurements of transport, diffusion and gas concentration have been organized by flow condition type in order to assess model accuracy. Operational models have not been found which are entirely suitable for NRC Regulatory predictive purposes. However, suggestions are made for model selection. Recommendations are also given for further research in areas where such efforts should prove profitable. It is concluded that the need is great for field scale measurements for model development and testing.

CONTENTS

		PAGE
SECTION 1.0	INTRODUCTION	15
SECTION 2.0	OBSERVATIONS OF FLOW AND MIXING PROPERTIES OF RELATIVELY DENSE GASES FOR NEAR-FIELD CONDITIONS	17
2.1	General	17
2.2	Near-Calm, Very Stable Atmosphere	19
2.3	Over Large Bodies of Water	21
2.4	Positively or Negatively Buoyant Elements	22
2.5	In the Lee of Obstacles to Flow	55
2.6	On or Near Highways	79
2.7	Irregular and Rugged Terrain	79
2.8	Over Cities	79
2.9	Very Close to the Source	80
SECTION 3.0	MODELS OF FLOW AND DIFFUSION OF DENSE GAS IN THE ATMOSPHERIC BOUNDARY LAYER	81
3.1	Properties of Gasflows which are to be Modeled	81
3.2	Recommended Interim Models	82
3.3	Jets and Gravity Currents	86
3.4	Factors in Choosing a First Order Model	89
SECTION 4.0	INTERIM METHODS FOR ESTIMATING CONCENTRATION	91
4.1	Three Possible Methods	91
4.2	A Modified Gaussian Plume-Puff Model	92

CONTENTS (cont.)

4.3	Simple Gravity Current or Jet Model	93
4.4	Computer Solutions of the Coupled Equations of Motion	96
4.5	Realistic Conditions for Application of the Basic Models	99
SECTION 5.0	RECOMMENDATIONS FOR NEEDED RESEARCH AND DEVELOPMENT	101
SECTION 6.0	CONCLUSIONS	105
REFERENCES		107

TABLES

Table		PAGE
1	Ranges of distance exponent value and ratios of measured-to-calculated concentrations by terrain class (data from Van der Hoven, 1976)	20
2	Flammability characteristics of hydrogen and methane (from Van Dolah, 1963)	29
3	Observations from accidental releases of heavy gases into the atmosphere (compiled from Eisenberg, Lynch and Breeding, 1975)	48
4	Some comparative properties of air, ammonia, chlorine, and methane	81

ILLUSTRATIONS

Figure		PAGE
1.	Relationship between day and night concentration ratios and water-air temperature difference ($^{\circ}F$). Concentrations evaluated for a point 0.5 miles from source. Overwater concentrations data based on overwater travel of 7 miles (adapted from Slade, 1962).	23
2.	Estimates of overwater-overland concentration ratio based on stability-to-concentration relationship: (a) Chesapeake Bay in vicinity of Chesapeake Bay Bridge, (b) Los Angeles-Long Beach, Calif., harbor area, (c) Duluth, Minn., harbor area (adapted from Slade, 1962).	24
3.	Measured values of instantaneous σ_y from overwater smoke plume photographs under stable and unstable conditions compared with Pasquill predictions (adapted from Raynor et al, 1975).	25
4.	Measured values of instantaneous σ_z from overwater smoke plume photographs under stable and unstable conditions compared with Pasquill predictions. The square represents a single aircraft observation (adapted from Raynor et al, 1975).	25
5.	Concentration per unit spill rate times wind velocity as a function of downwind distance for continuous spills on water (adapted from Gideon and Putnam, 1976).	27
6.	Normalized concentration - wind velocity product as function of distance for instantaneous spills (sensor data unless otherwise noted). A is area of water spill (adapted from Gideon and Putnam, 1976).	27
7.	Relation between concentrations measured by sensors and calculated from fog dispersal (adapted from Gideon and Putnam, 1976).	28
8.	Extent of the flammable mixtures and height of the visible cloud formed after the rapid spillage of 3 liters of liquid hydrogen on a dry macadam surface in a quiescent air atmosphere at $59^{\circ}F$ (adapted from Van Dolah, 1963).	30
9.	Extent of flammable zone above downwind dike following spillage of LNG (from Van Dolah, 1963).	31
10.	Sequence of areal extent and location for a Freon 12 spill based on measurements (adapted from Van Ulden, 1974).	33

11. Measured vertical spread of cloud vs time in early stages after the spill (adapted from Van Ulden, 1974). 34

12. Vertical spread of cloud vs distance during later stages after spill (adapted from Van Ulden, 1974). 35

13. Lateral spread of cloud vs distance (adapted from Van Ulden, 1974). 35

14. Rate of entrainment, E, into a turbulent stratified flow as a function of overall Richardson number, for two types of experiment described by Ellison and Turner (1959), and the experiments of Lofquist (1960) (adapted from Turner, 1973). 37

15. Measurements of entrainment into an inclined plume as a function of slope (adapted from Turner, 1973). 37

16. Sketch of a gravity current on a slope, with an initial head followed by a steady layer flow (adapted from Turner, 1973). 38

17. Peak concentration correlation with distance from spill. Values of variables scaled to prototype magnitudes (from Neff et al, 1976). 40

18. Low dike gas release rates for model and prototype (from Neff et al, 1976). 41

19. Dimensionless concentration coefficients vs non-dimensional downwind distance for stability class C (from Neff et al, 1976). 42

20. Dimensionless concentration coefficient vs non-dimensional downwind distance for stability class F (from Neff et al, 1976). 43

21. Visualization of plume from low dike model - wind direction 45° (adapted from Neff et al, 1975). 44

22. Side-view of a plume, which is very dense (about 4x air), bending downwind and earthward from its source stack (from Hoot et al, 1973). 45

23. Maximum concentration vs downstream distance, plumes in a laminar crosswind, R = 15, D_o = 1/8 inch, $\bar{x}$ = horizontal distance to plume high point (adapted from Hoot et al, 1973). 46

24. Velocity profiles in law of the wall coordinates near a smooth solid wall for varying stability. The scale of the abscissa is logarithmic. The position of the logarithmic line is displaced upward under stable conditions and downward under unstable conditions. Stability is characterized by a bulk boundary layer Richardson number, as illustrated (from Csanady, 1978). 54

25. Experimental data of Wu in modified law of the wall coordinates (from Csanady, 1978). 54

26. Relative concentrations normalized by windspeed as a function of distance for (a) field and wind tunnel tests during stable conditions, (b) field tests during unstable-neutral conditons, and (c) wind tunnel tests during unstable-neutral conditons. Pasquill F and D curves are shown for comparison (adapted from Abbey, 1976). 58

27. Centerline concentration vs downwind distance for lapse conditions (from Dickson et al, 1969). 59

28. Centerline concentrations vs downwind distance for inversion conditions (from Dickson et al, 1969). 60

29. K-mean isopleths of effluent released from containment building during inversion conditions (from Dickson et al, 1969). 62

30. K-maximum isopleths of effluent released from containment building during inversion conditions (from Dickson et al, 1969). 63

31. Halitsky's wind tunnel K-isopleths for neutral release (from Dickson et al, 1969). 64

32. Isopleths of exposure (normalized to source strength) for the test series, with position of the self-orienting- real-time-sampler (SORTS) indicated by + (adapted from Hinds, 1969). 65

33. Topography of the Rancho Seco study site, showing the details of terrain that influenced the measured concentrations. Heights are feet above sea level (from Start et al, 1977). 66

34. Plotplan of Rancho Seco study site, indicating sampler positions (from Start et al, 1977). 68

35. Mean ratios for calculated (observed) sigma-y values divided by expected Pasquill-Gifford values. * denotes the mean ratios for each distance. The line is a regression fit of the mean values (adapted from Start et al, 1977). 69

36. Mean ratios for calculated (observed) sigma-z values divided by expected Pasquill-Gifford values (adapted from Start et al, 1977). 69

37. Mean ratios for Pasquill-Gifford values divided by observed maximum concentration values (adapted from Start et al, 1977). 70

38. Comparison of averaged normalized maximum concentrations at each downwind arc and calculated normalized peak concentrations. Calculated values use Pasquill- Gifford sigma values plus an added term to incorporate an effect due to building cross sectional area for stabilities D - F (adapted from Start et al, 1977). 70

39. Concentration isopleths ($X\bar{u}/Q$ in negative powers of ten) for F12, test 4. Tracer was released from surface positions G5 under NRC stability category G. Mean tower wind at release height was from 038 degrees at 1.3 m/s (from Start et al, 1977). 71

40. Concentration isopleths ($X\bar{u}/Q$ in negative powers of ten) for SF6, test 8. Tracer was released at auxiliary building roof under NRC stability category G. Mean tower wind at release height was from 110 degrees at 2.5 m/s (from Start et al, 1977). 72

41. Concentration isopleths ($X\bar{u}/Q$ in negative powers of ten) for F12, test 10. Tracer was released at surface position G5 under NRC stability category F. Mean tower wind at release height was from 330 degrees at 3.0 m/s (from Start et al, 1977). 73

42. Concentration isopleths ($X\bar{u}/Q$ in negative powers of ten) for SF6, test 10. Tracer was released at auxiliary building roof under NRC stability category F. Mean tower wind at release height was from 346 degrees at 4.9 m/s (from Start et al, 1977). 74

43. $\theta = 0^{o}$, bottom exit port, neutral stratification (from Yang and Meroney, 1970). 76

44. $\theta = 0^{o}$, middle exit port, neutral stratification (from Yang and Meroney, 1970). 76

45. $\theta = 0^{o}$, bottom exit port, inversion stratification (from Yang and Meroney, 1970). 77

46. $\theta = 0^{o}$, middle exit port, inversion stratification (from Yang and Meroney, 1970). 77

47. Lateral profiles of turbulence intensity excess in the wake of the building at 0 degrees (adapted from Hansen et al, 1974). 78

48. Lateral profiles of turbulence intensity excess in five heights above the ground on tower 3-1/2 (adapted from Hansen et al, 1974). 78

49. Five basic models representing first approximations to Cl_2, NH_3, and CH_4 accidental release, transport and diffusion. 83

50. A schematic composite of a higher-order-approximation model of transport and diffusion in a hazardous gas accident. 85

51. A side view sketch of a steady gravity current on a slope (adapted from Turner, 1973). 87

52. A speed profile for a heavy layer flowing laminarly down a smooth slope (adapted from Turner, 1973). 87

53. Cross section plots of concentration of heavy gas plume, $(XUD_o^2/Q) \times 10^4$ (from Hoot et al, 1973). 94

54. Maximum concentration vs downstream distance of plumes in a laminar crosswind, R = 5, D_o= 1/8 inch, $\bar{x}$ = horizontal distance to plume high point (adapted from Hoot et al, 1973). 95

55. Non-dimensional, normalized plot for various release heights showing decay of plume maximum concentration downstream from touchdown point in turbulent boundary layer. h_s= stack height, H = plume height, Z_o= roughness length U_∞= free stream velocity, Q = emission rate, x = distance downstream, and X = concentration (adapted from Hoot et al, 1973). 97

56. Velocity field at 20 s after start of calculation shows large recirculation in a V shaped highway cut. Note that center of recirculation eddy is shifted downstream from the center of the cut (from Hirt et al, 1975). 98

57. Vertical profiles of (a) vertical wind speed and (b) horizontal wind speed upwind and downwind of a 2-d ridge computed by a simplified marker and cell technique (from Connell, 1976). 100

RECOMMENDED METHODS FOR ESTIMATING ATMOSPHERIC CONCENTRATIONS OF HAZARDOUS VAPORS AFTER ACCIDENTAL RELEASE NEAR NUCLEAR REACTOR SITES

SECTION 1.0 Introduction

The following literature survey and evaluation address the problems of transport and diffusion of gas with the special conditions that (1) the gas is either significantly heavier or lighter than ambient air, (2) the gas is near its source region (the near field) and (3) the flow may be influenced by rough and complex surface terrain or by buildings. The objective was to determine the state of the art for the analysis of hazards to nuclear power plants. Fire and explosion hazards are not specifically considered here. Similar surveys and evaluations of the diffusion and transport literature have been made previously for other purposes and are included here in a condensed form.

The problem of near-field transport and diffusion, especially of positively or negatively buoyant gas volumes in air, is complex and mostly unsolved. Valid physical models have yet to be constructed and tested. A few computer simulations, fluid laboratory, and field-scale measurements have been made. They provide a basis from which to continue the learning process but are inadequate for setting up decision-making criteria related to hazardous gas effects at nuclear reactor sites. Three gases are taken to represent potential hazards: chlorine, ammonia, and liquified natural gas (LNG) vapor.

Models which have predictive capabilities for conditions at

specific sites fall in the following categories:

(1) Analytical solutions to parameterized steady state or time averaged diffusion equations for the far field from fixed sources (e.g., Gaussian models of dispersion).

(2) Continuity-transport equations solved by finite difference or finite element iterative schemes (kinematic).

(3) Coupled mass and motion equations solved by finite difference or finite element iterative schemes or, more rarely, by spectral methods (dynamic).

(4) Fluid laboratory simulations using scaling relationships and special "meteorological tunnels."

This literature survey presents selected measurements of atmospheric transport and diffusion from both field and laboratory experiments. Evaluations are also presented of model capabilities to simulate these observed atmospheric properties. These evaluations involve the adequacy of physical process description, and comparison of resulting effluent concentration fields with measurements.

The report also discusses pertinent observations relative to flows of dense gases in near-field conditions. Most observations are for neutral or near-neutral stability classes. Flow and mixing situations subdivided into eight special categories that depart from simple uniform flows are discussed in Section 2. Section 3 concentrates on the dense gas case, while Section 4 discusses three basic concepts for interim methods for estimating concentrations. Section 5 points out areas of research and development necessary for the formulation of adequate transport and diffusion models. Section 6 summarizes the report and its conclusions.

SECTION 2.0 Observations of Flow and Mixing Properties of Relatively Dense Gases for Near-Field Conditions

2.1 General

Existing observations of the flow and mixing of a dense gas close to the region of initial release provide a basis for evaluating the state of physical-mathematical modeling of the concentration distribution of hazardous, dense gas following its accidental release. Gifford (1976) reviewed current Gaussian plume methods of estimating diffusion of nonbuoyant tracers using typing schemes such as the Pasquill-Gifford (P-G) stability categories. He noted that existing models dependent on typing schemes were designed for specific conditions:

(1) Mean wind speeds greater than 2 m/s

(2) Nonbuoyant plumes

(3) Boundary layer flow over uniform open countryside containing few if any rough or blunt obstacles of large dimensions

(4) Turbulent mixing caused solely by boundary layer mechanical and thermal convective processes

(5) A distance of 100 m to 1 km from a source of small dimensions

However, there are many common flow conditions in the atmosphere which differ significantly from those specified for the modeling scheme. Gifford lists the following flow situations as exceptions:

(1) Near-calm, very stable atmosphere

(2) Over large bodies of water

(3) Positively or negatively buoyant elements (the principle area of concern in this report)

(4) In the lee of obstacles

(5) On and near highways

(6) Over irregular and rugged terrain

(7) Over cities

(8) Very close to the source

Under appropriate conditions, the Gaussian plume methods may lead to concentration estimates accurate to within 20% for long time averages. However, even if the applicable conditions for Gaussian plume methods do exist, most accidental hazardous gas releases of relevance will not result in long exposure times to the nuclear power plant. Gifford (1960) estimated that these methods may be in error by as much as 200% for short-time averages. The division between long and short times may be considered to be about 30 minutes. If more accurate estimates under these special conditions are required, or if other initial and boundary conditions are appropriate, then different methods of estimation are required. In citing the following field and laboratory experiments, the question of data quality and applicability to the above problem areas arises. The task of properly determining such quality, while highly desirable, is beyond the scope of this review.

This review is not exhaustive, but discusses a representative class of flow problems which have been studied. The data provide a basis for the evaluation and recommendation of models for use in

estimating the type and severity of hazards to nuclear power plant personnel and facilities from gas releases.

2.2 Near-calm, Very Stable Atmosphere

Field measurements of atmospheric diffusion under low wind speed inversion conditions were surveyed by Van der Hoven (1976). The measurements were made at distances of up to 2 km from a single source, at three different types of sites:

(1) A broad flat valley with sparse low vegetation surrounded by mountain ranges (two sites)

(2) A broad flat valley containing forest interspersed with cultivated fields (one site), and a partially wooded island in a river with wooded hills rising 80 m above the river within 3 km of the gas release point (one site)

(3) A complex terrain site, thickly wooded, with ridges, rising to 100 m above the release point and including a horseshoe bend in a river, that bounded the release point on three sides within 600 to 1200 m

Gas tracer releases at all sites were of 30 to 60 minutes duration and generally were incorporated into the ambient air in low concentrations near the source. Tracer gas buoyancy, therefore, was not a consideration. Sampling times ranged from about 20 to 60 minutes. Measurements of tracer concentration were made at the surface and, in a few cases, from towers up to 9 m above the local ground.

Atmospheric conditions were classified by the P-G scheme as type

E, F, or G. All observed concentrations differed considerably from those calculated with a Gaussian model using the P-G typing scheme. For example, in flat terrain, the upper bound envelope of concentration ratios was

$$\frac{X_{measured}}{X_{calculated}} < 0.43\ (E),\ 0.77\ (F),\ 0.28\ (G),$$

where X is peak concentration at the ground at a given distance.

Another measure of the departure from Gaussian model behavior and P-G typing is given by the downwind decrease of the maximum center line normalized concentration,

$$Xu/Q = bx^p \qquad (1)$$

where u is mean wind speed, Q is source strength, b is a constant, and x is distance from the source. The observed ranges of value of the exponent, p, are shown in Table 1.

TABLE 1.

Ranges of Distance Exponent Value and Ratios of Measured-to-Calculated Concentrations by Terrain Class (data from Van der Hoven, 1976)

Terrain Type	Ranges of Exponent Values	$\frac{X_{measured}}{X_{calculated}}$
Smooth Terrain	p = -0.5 to -0.8	0.77 to 0.28
Flat Forest	p = -1.5 to -1.7	0.50 to 0.25
Hilly Forest	p = -2.0 to -2.4	0.002 to 0.02

Regression lines representing the observed concentration decay with distance, expressed by equation (1), indicated far smaller concentrations than did the P-G estimates as shown in the third column.

Peak concentrations at 150 m to 250 m from the tracer source were found to exist within 6 m of the surface. Sometimes multiple concentration peaks were observed in the cross wind direction. At a distance of 200 m the plume was about 70 m wide. At x = 1000 m and 1 hour of sampling, multiple peaks were observed even with 10 m sampler spacing.

A modification to the stability classification scheme to include terrain influences for type E, F, and G was attempted. The resulting calculated Gaussian plume concentration estimates showed little improvement when compared to the measurements. Flow irregularities were apparently so great that use of a Gaussian scheme became inappropriate.

2.3 Over Large Bodies of Water

Only a few useful documented observations of transport and diffusion over water were found. All of those examined involved tracer gases of near-neutral buoyancy under different atmospheric stratification conditions.

Slade (1962) estimated standard deviations of horizontal wind direction, σ_θ, from wind direction measurements made on both shores of Chesapeake Bay. With the wind from the west, this arrangement provided long upwind fetches over water for one case and over land for another. Values of lateral and vertical plume spread, σ_y and σ_z, were made which

allowed application of the Gaussian plume centerline concentration. The series of calculated overwater-to-overland concentration ratios, X_W/X_L, at a fixed distance from a point source of airflow indicated much weaker diffusion over water than over land for wind speeds from 5 to 8 m/s. Figure 1, from Slade's paper, shows estimated relationship between day and night concentration ratios of plumes as a function of water-air temperature difference. Figure 2 shows the distribution of X_W/X_L with time of day and year.

Raynor et al (1975) showed that the spread and concentration of a neutrally buoyant plume having a 2 to 5 km fetch over water is primarily a function of air-water temperature difference. Instantaneous values of observed σ_y and σ_z are much smaller than those predicted by the P-G curves (Figures 3 and 4). It was necessary to measure rms values of lateral and vertical wind fluctuations, σ_v and σ_w, in order to adequately estimate the plume spreads, σ_y and σ_z.

Much scatter in the data suggests a need to consider surface roughness and buoyancy mechanisms as modified by surface waves, heat, and water vapor. Gifford (1976) has surveyed some of the applicable concepts.

Luna and Church (1972) suggested that, even over land, wind direction fluctuation does not correlate well with the P-G curves because there is so much scatter that almost any σ_θ, σ_ϕ may be associated with any stability class.

2.4 Positively or Negatively Buoyant Elements

Field experiments which provide measurements of concentration distributions of a buoyant gas intrusion are sparse. In reviewing some

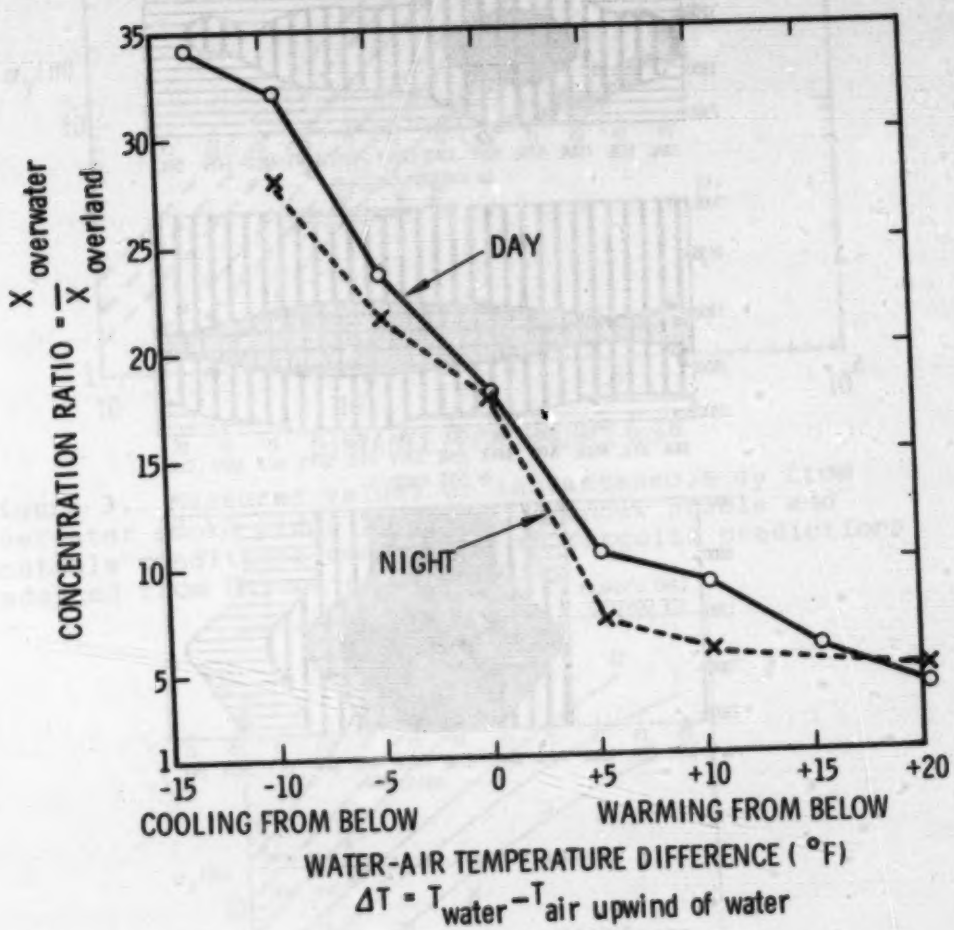

Figure 1. Relationship between day and night concentration ratios and water-air temperature difference (°F). Concentrations evaluated for a point 0.5 miles from source. Overwater concentrations data based on overwater travel of 7 miles (adapted from Slade, 1962).

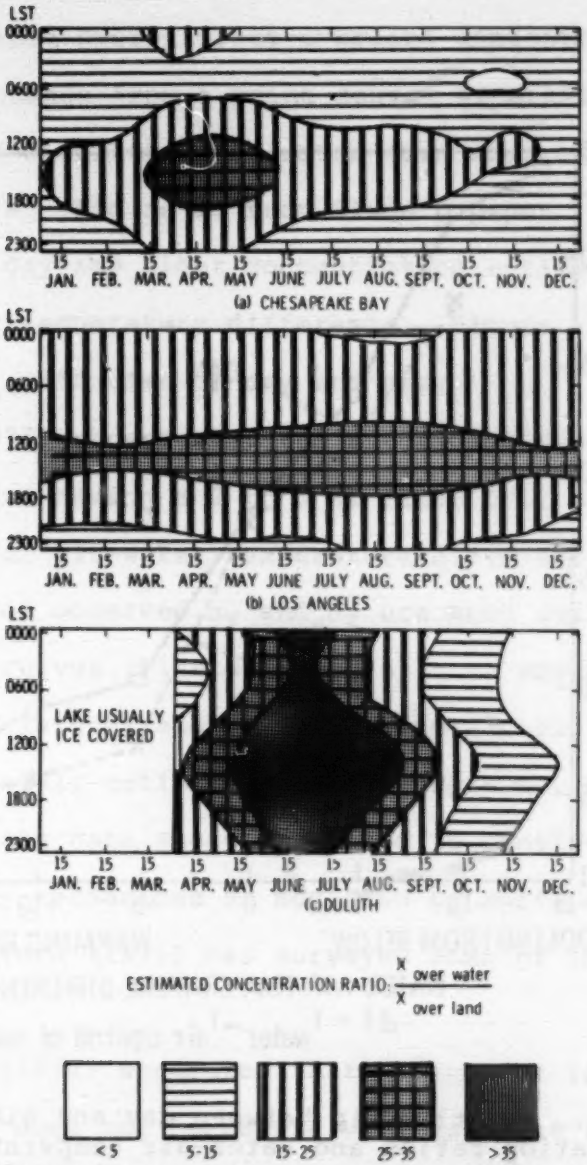

Figure 2. Estimates of overwater-overland concentration ratio based on stability-to-concentration relationship: (a) Chesapeake Bay in vicinity of Chesapeake Bay Bridge, (b) Los Angeles-Long Beach, Calif., harbor area, (c) Duluth, Minn., harbor area (adapted from Slade, 1962).

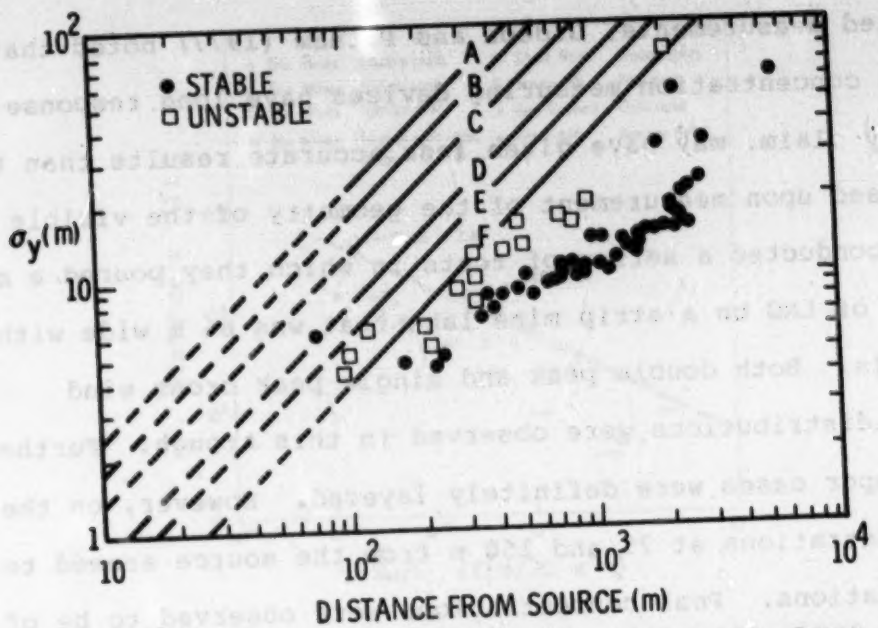

Figure 3. Measured values of instantaneous σ_y from overwater smoke plume photographs under stable and unstable conditions compared with Pasquill predictions (adapted from Raynor et al, 1975).

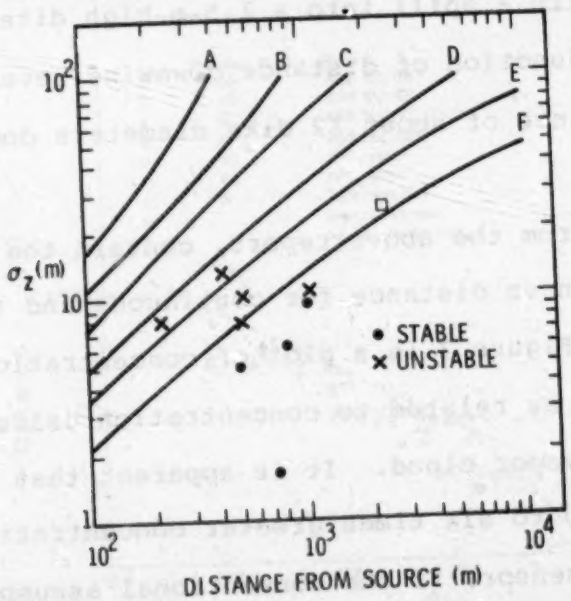

Figure 4. Measured values of instantaneous σ_z from overwater smoke plume photographs under stable and unstable conditions compared with Pasquill predictions. The square represents a single aircraft observation (adapted from Raynor et al, 1975).

of the reported measurements, Gideon and Putnam (1977) noted that most available gas concentration measuring devices have long response times, and thus, they claim, may have given less accurate results than those calculated based upon measurement of the geometry of the visible vapor cloud. They conducted a series of tests in which they poured a maximum of about 9 m^3 of LNG on a strip mine lake that was 66 m wide with steep 18 m high walls. Both double peak and single peak cross wind concentration distributions were observed in this trough. Further, the single peak vapor cases were definitely layered. However, on the average, concentrations at 75 and 150 m from the source seemed to fit the P-G calculations. Peak concentrations were observed to be of greater magnitude in slight wind than for no wind. No explanation was given for this result.

In another test with a spill into a 1.5-m-high diked area, a plot of concentration as a function of distance downwind revealed a marked slope change at a distance of about 12 dike diameters downwind in a 2.2 m/s wind.

Figures 5 and 6, from the above report, contain the data for normalized concentration vs distance for continuous and instantaneous spills, respectively. Figure 7 is a plot of concentration of methane measured by gas sensors as related to concentration calculated by noting the size of the vapor cloud. It is apparent that the visual boundary method gives up to six times greater concentration than does measurement with a gas sensor, if the conventional assumption that the visible edge is at 0.1 the peak value is made. It is felt by the present authors that this may not result so much from slow instrumental

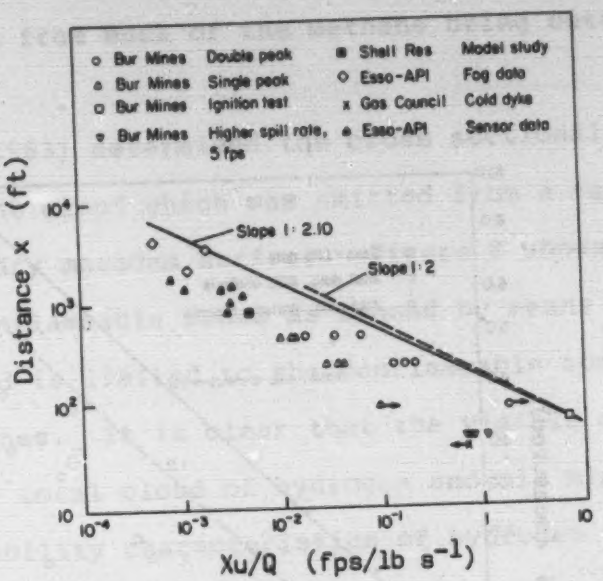

Figure 5. Concentration per unit spill rate times wind velocity as a function of downwind distance for continuous spills on water (adapted from Gideon and Putnam, 1976).

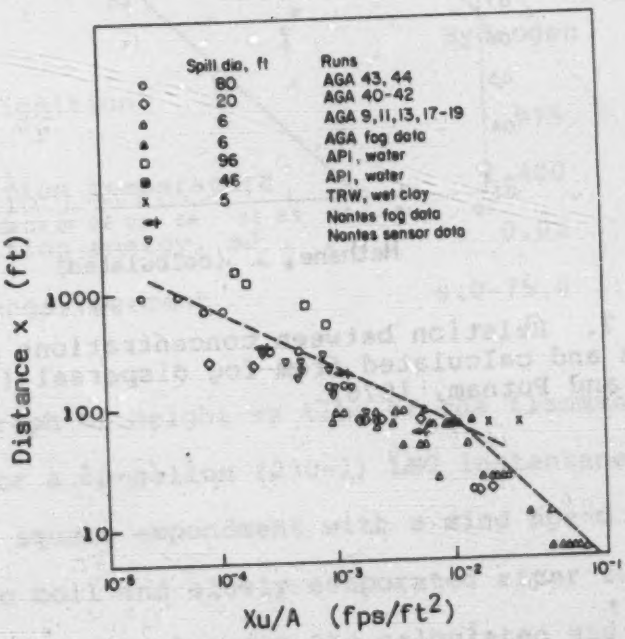

Figure 6. Normalized concentration - wind velocity product as function of distance for instantaneous spills (sensor data unless otherwise noted). A is area of water spill (adapted from Gideon and Putnam, 1976).

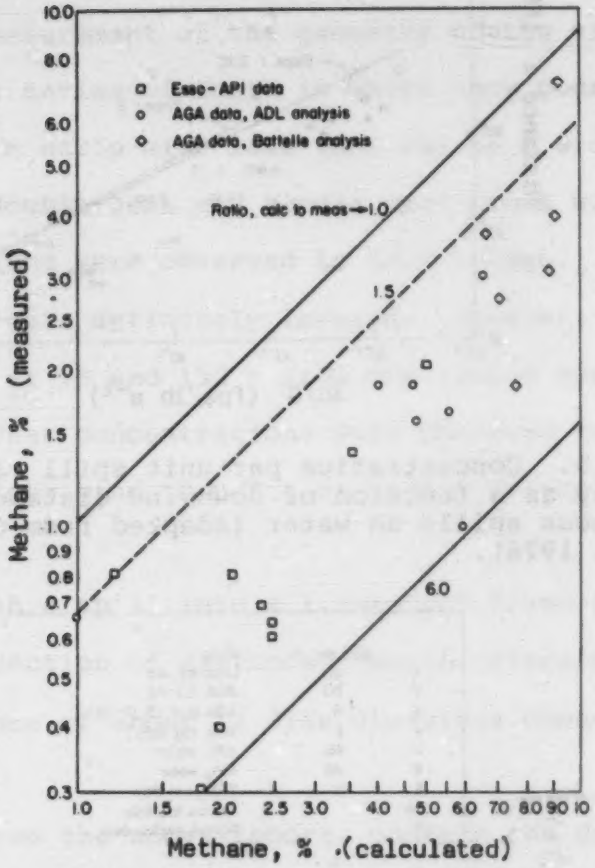

Figure 7. Relation between concentrations measured by sensors and calculated from fog dispersal (adapted from Gideon and Putnam, 1976).

response time, as from much of the methane being outside the visible cloud boundary.

Van Dolah (1963) determined the cross sectional shape of a positively buoyant cloud which was emitted from a rapid spill of liquid hydrogen onto a dry macadam surface. Figure 8 shows height of the flammable and nonflammable zones as sensed by means of various probes. The visible cloud is limited to the nonflammable zone enclosed within the flammable zones. It is clear that the visible cloud is much smaller than the total cloud of hydrogen and air mixture. Table 2 gives the flammability characteristics of hydrogen and methane.

TABLE 2

Flammability Characteristics of Hydrogen and Methane
(from Van Dolah, 1963.)

	Hydrogen	Methane
Spontaneous ignition temperature, °F	975	1,000
Hot gas ignition temperature	1,400	2,420
Minimum ignition energy, mJ	0.02	0.3
Flammable range, percent	4.0-75.0	5.0-14.0

Figure 9 is a graph of height vs time of the flammable zone above a downwind dike for a 60-gallon (230-l) LNG instantaneous spill into a 5-foot-(1.5-m-) square empondment with a wind speed of 5 m/s. The liquid ceased to boil and slowly evaporated after two minutes. The quality of the agreement between the calculated and experimental value can be assessed from the figure.

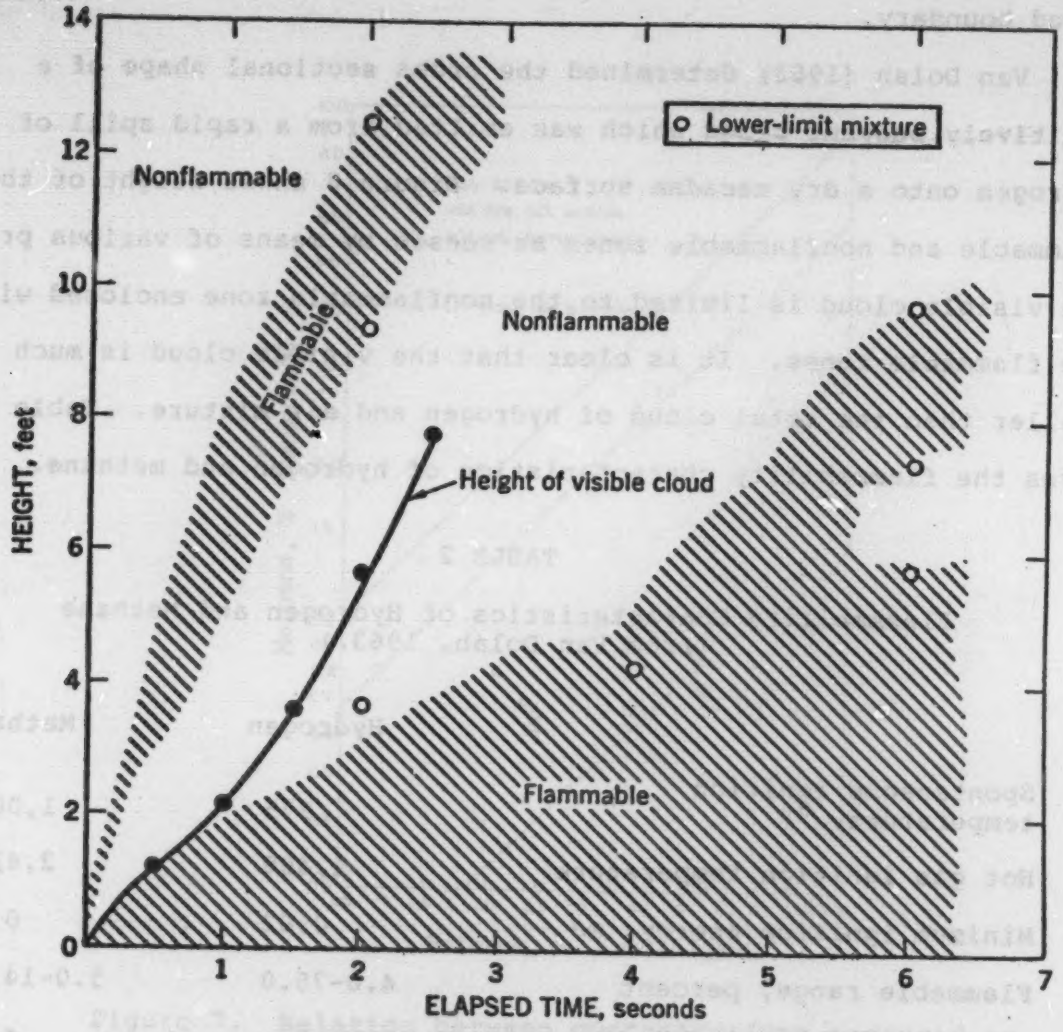

Figure 8. Extent of the flammable mixtures and height of the visible cloud formed after the rapid spillage of 3 liters of liquid hydrogen on a dry macadam surface in a quiescent air atmosphere at 59°F (adapted from Van Dolah, 1963).

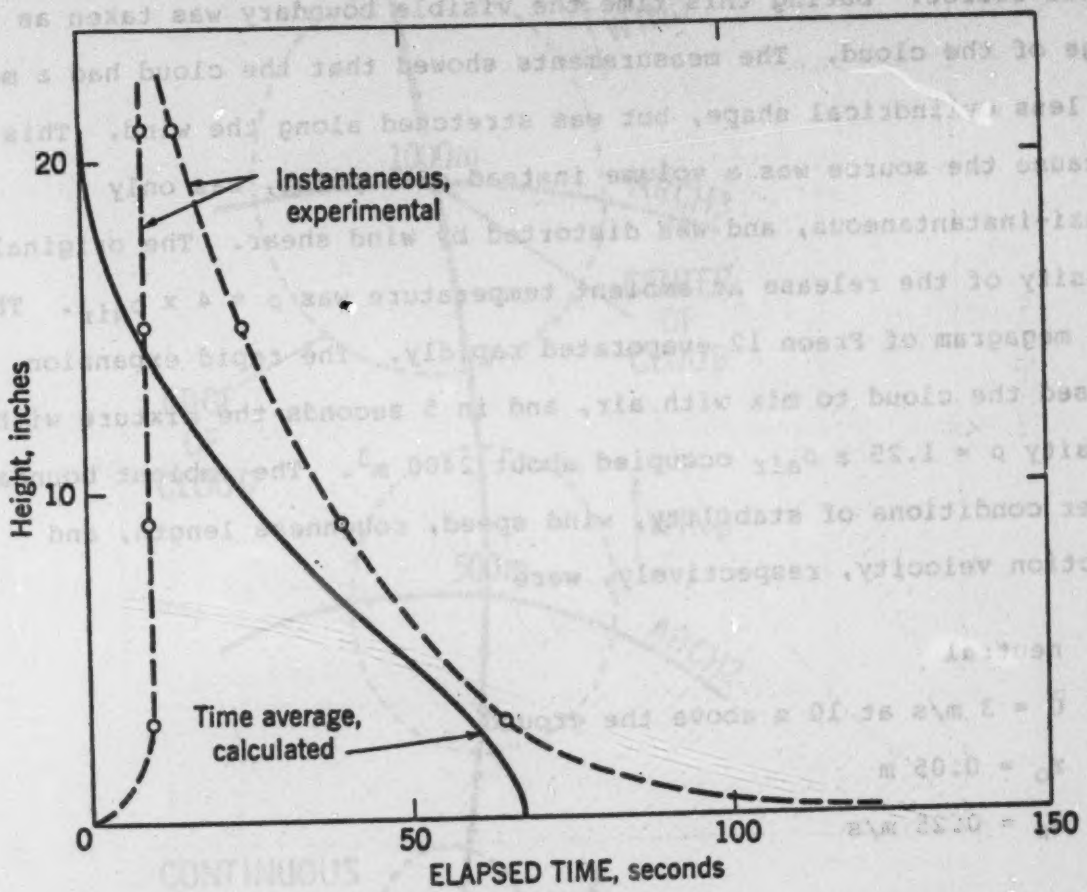

Figure 9. Extent of flammable zone above downwind dike following spillage of LNG (from Van Dolah, 1963).

Van Ulden (1974) measured the spread and translation of an initially visible cloud caused by a Freon 12 spill. The cloud was visible with distinct boundaries for about 40 s or up to 30 m from the spill source. During this time the visible boundary was taken as the edge of the cloud. The measurements showed that the cloud had a more or less cylindrical shape, but was stretched along the wind. This is because the source was a volume instead of a point, was only quasi-instantaneous, and was distorted by wind shear. The original density of the release at ambient temperature was $\rho = 4 \times \rho_{air}$. The one megagram of Freon 12 evaporated rapidly. The rapid expansion caused the cloud to mix with air, and in 5 seconds the mixture with density $\rho = 1.25 \times \rho_{air}$ occupied about 2400 m^3. The ambient boundary layer conditions of stability, wind speed, roughness length, and friction velocity, respectively, were

neutral

$\bar{U} = 3$ m/s at 10 m above the ground

$z_o = 0.05$ m

$u_* = 0.25$ m/s

Figure 10 shows the sequence of location and areal extent of the cloud based on Freon 12 sampler measurements. Figure 11 shows the photographically measured height of the top of the cloud during the initial spreading stage. Figure 12 shows the height of the top of the cloud out to a distance of 1000 m. Although diffusion was significant, density effects very effectively reduced the vertical spread. Figure 13 shows the lateral spread of the cloud. Note that the Gaussian model

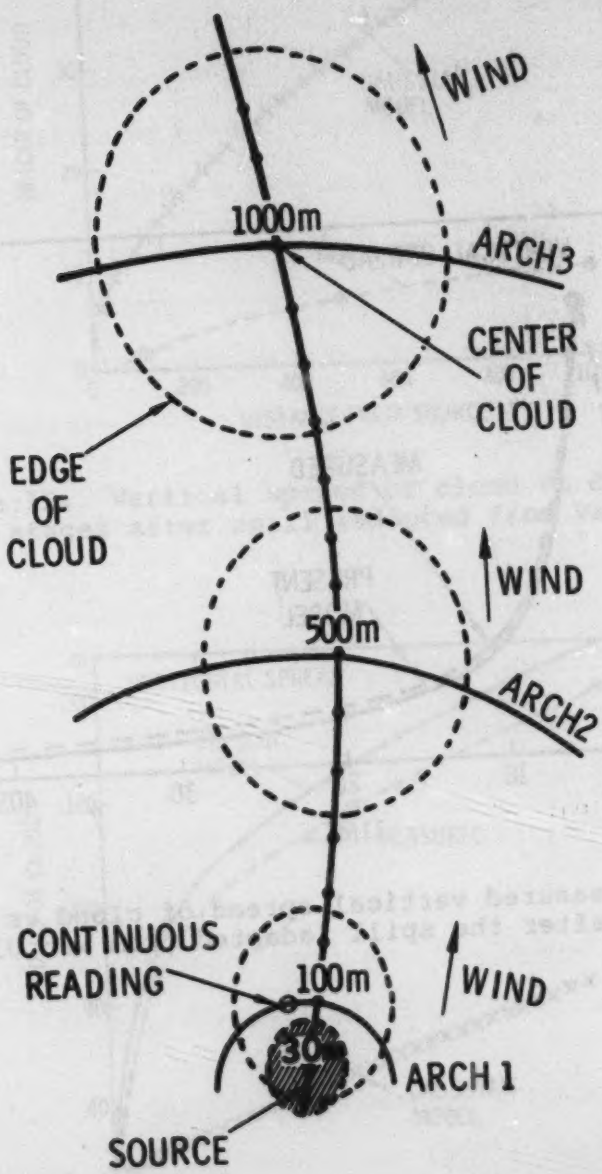

Figure 10. Sequence of areal extent and location for a Freon 12 spill based on measurements (adapted from Van Ulden, 1974).

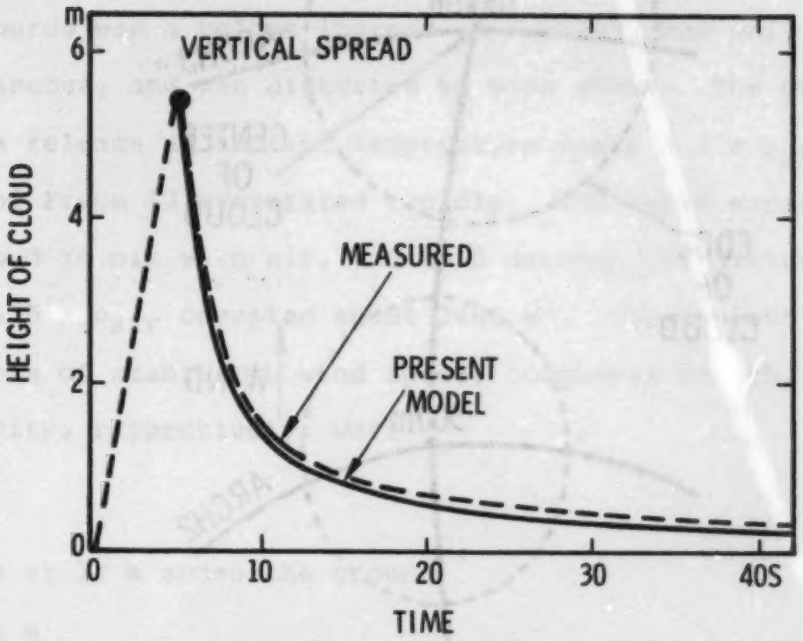

Figure 11. Measured vertical spread of cloud vs time in early stages after the spill (adapted from Van Ulden, 1974).

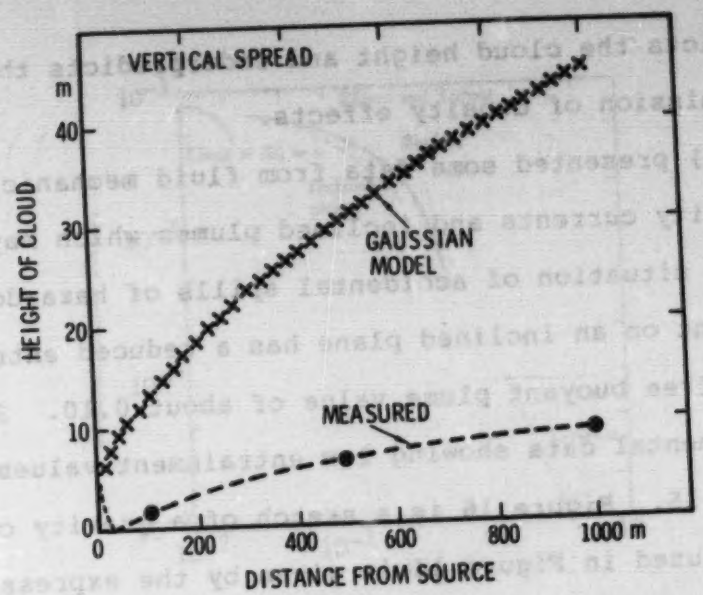

Figure 12. Vertical spread of cloud vs distance during later stages after spill (adapted from Van Ulden, 1974).

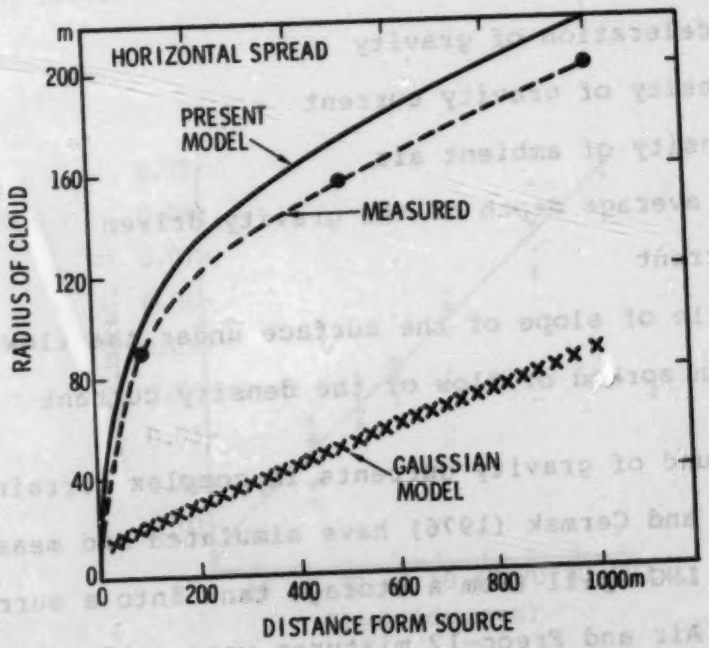

Figure 13. Lateral spread of cloud vs distance (adapted from Van Ulden, 1974).

grossly overpredicts the cloud height and underpredicts the cloud width because of its omission of density effects.

Turner (1973) presented some data from fluid mechanics experiments on turbulent gravity currents and inclined plumes which may be applicable to the situation of accidental spills of hazardous gases. The gravity current on an inclined plane has a reduced entrainment rate as compared to a free buoyant plume value of about 0.10. Some summarized experimental data showing low entrainment values are shown in Figures 14 and 15. Figure 16 is a sketch of a gravity current. The Richardson number used in Figure 14 is given by the expression

$$Ri_o = g' h \cos\theta / U^2$$

where

$g' = g(\rho_i - \rho)/\rho$

g = acceleration of gravity

ρ_i = density of gravity current

ρ = density of ambient air

h = an average depth of the gravity driven current

θ = angle of slope of the surface under the flow

U = mean spread of flow of the density current

No studies were found of gravity currents in complex terrain.

Neff, Meroney and Cermak (1976) have simulated and measured a negatively buoyant LNG spill from a storage tank into a surrounding diked empondment. Air and Freon-12 mixtures were used to simulate boiloff densities of methane, the principal component of LNG. A key

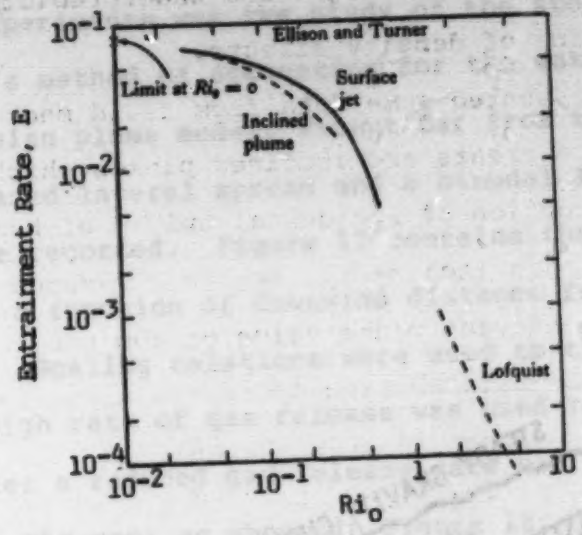

Figure 14. Rate of entrainment, E, into a turbulent stratified flow as a function of overall Richardson number, for two types of experiment described by Ellison and Turner (1959), and the experiments of Lofquist (1960) (adapted from Turner, 1973).

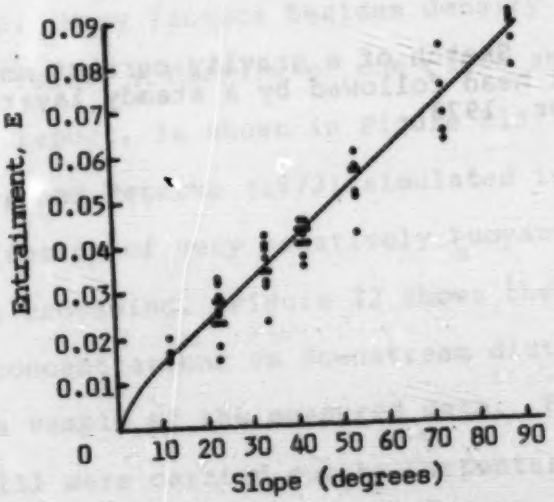

Figure 15. Measurements of entrainment into an inclined plume as a function of slope (adapted from Turner, 1973).

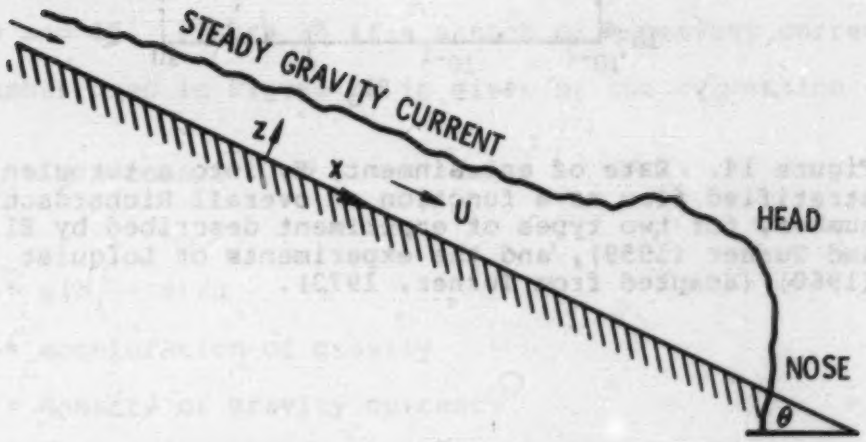

Figure 16. Sketch of a gravity current on a slope, with an initial head followed by a steady layer flow (adapted from Turner, 1973).

feature of the experiments was the study of the storage tank wake. However, Gifford's method of accounting for the wake was not successful nor was the Gaussian plume model, except far from the region of interest. Increased lateral spread and a bimodal lateral concentration distribution were recorded. Figure 17 contains the normalized plots of concentration as a function of downwind distance for several initial spill diameters. Scaling relations were used to transform distances to full scale. A high rate of gas release was used to simulate initial boiling, and later a reduced gas release rate was used to simulate evaporation from the pool as shown in Figure 18. The prototype times and rates shown were scaled up from the model values. Two examples of measured concentration, X, vs distance from spill center, x, are compared to Gaussian curves for stability categories C and F, respectively, in Figures 19 and 20. The values have been nondimensionalized by use of mean wind speed, $\bar{u}$, source strength, Q, and dike height, H. Many factors besides density of the released gas apparently play a role. A drawing of one plume shape, adapted from the Neff et al (1976) report, is shown in Figure 21.

Hoot, Meroney and Peterka (1973) simulated in a wind tunnel the transport and diffusion of very negatively buoyant plumes ejected vertically into a crosswind. Figure 22 shows the shape of one such plume. Maximum concentrations vs downstream distance were measured. Figure 23 gives a sample of the measured data. Further studies of simulated LNG spill were carried out by Carpenter et al (1978). However, the report was not available to the authors in time to be included here.

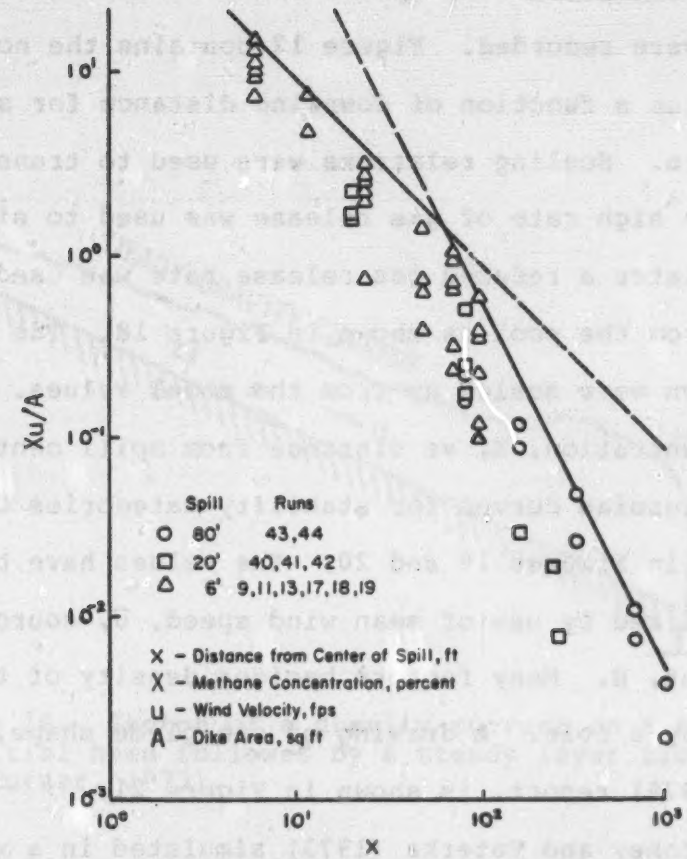

Figure 17. Peak concentration correlation with distance from spill. Values of variables scaled to prototype magnitudes (from Neff et al, 1976).

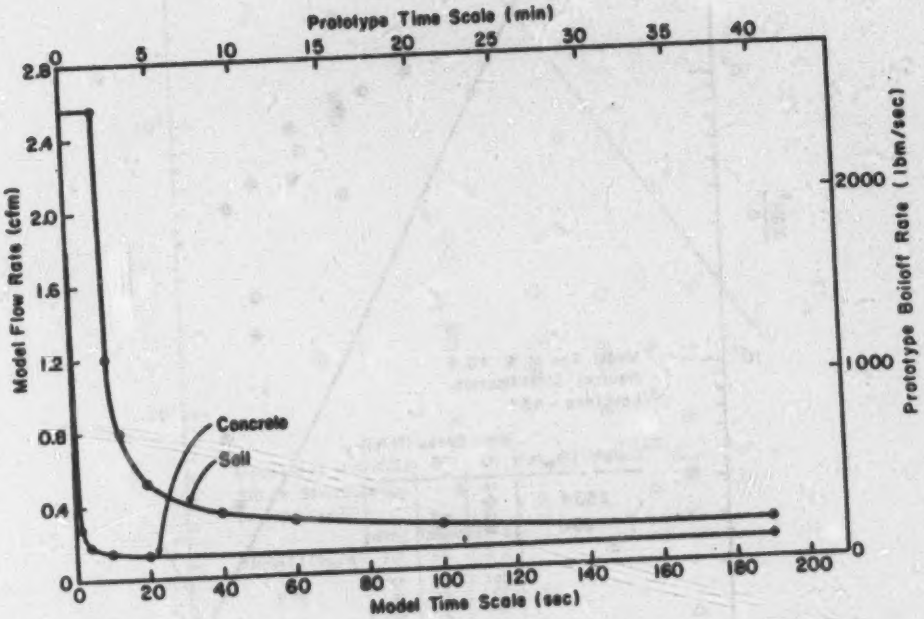

Figure 18. Low dike gas release rates for model and prototype (from Neff et al, 1976).

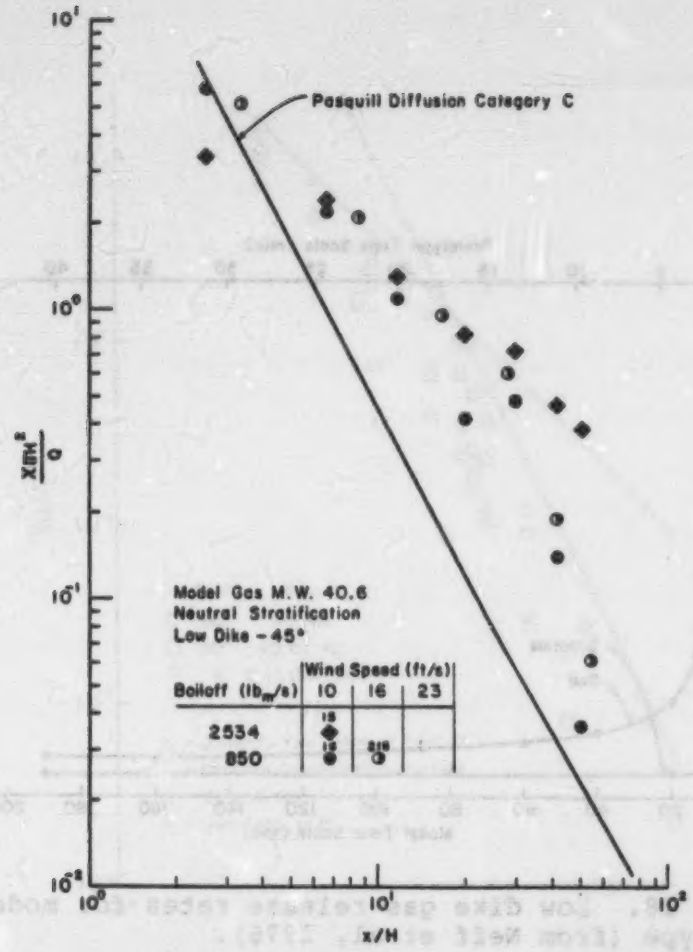

Figure 19. Dimensionless concentration coefficients vs non-dimensional downwind distance for stability class C (from Neff et al, 1976).

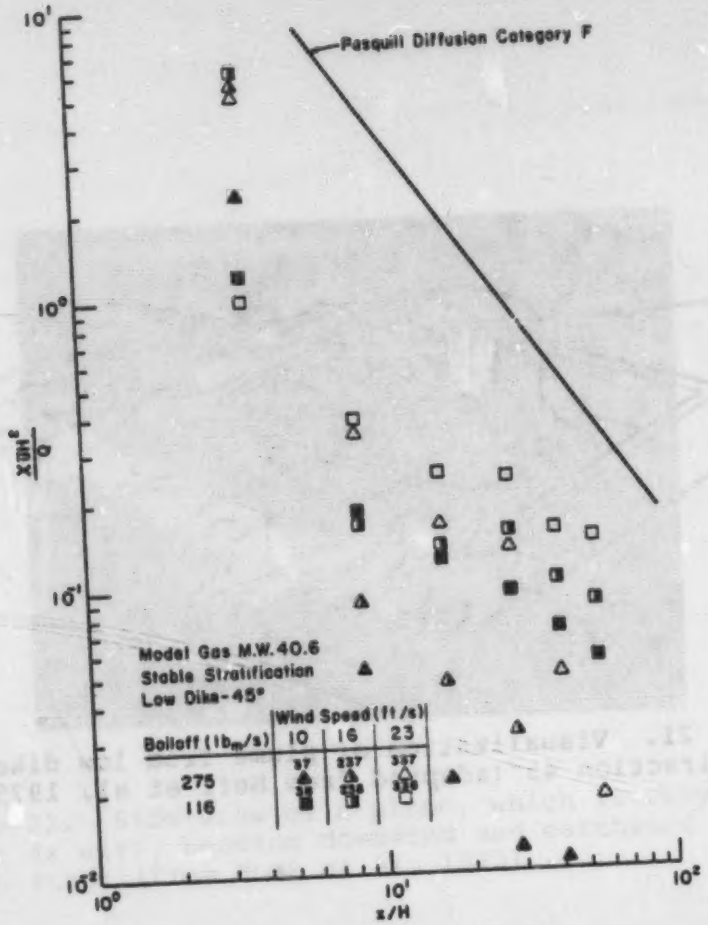

Figure 20. Dimensionless concentration coefficient vs non-dimensional downwind distance for stability class F (from Neff et al, 1976).

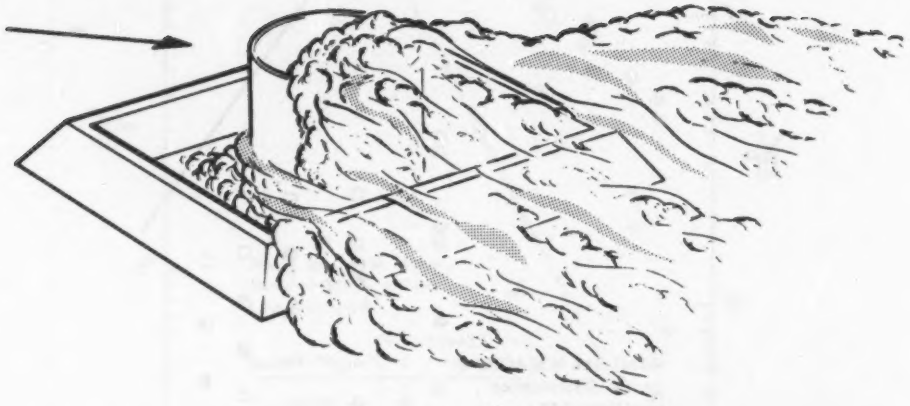

Figure 21. Visualization of plume from low dike model - wind direction 45° (adapted from Neff et al, 1975).

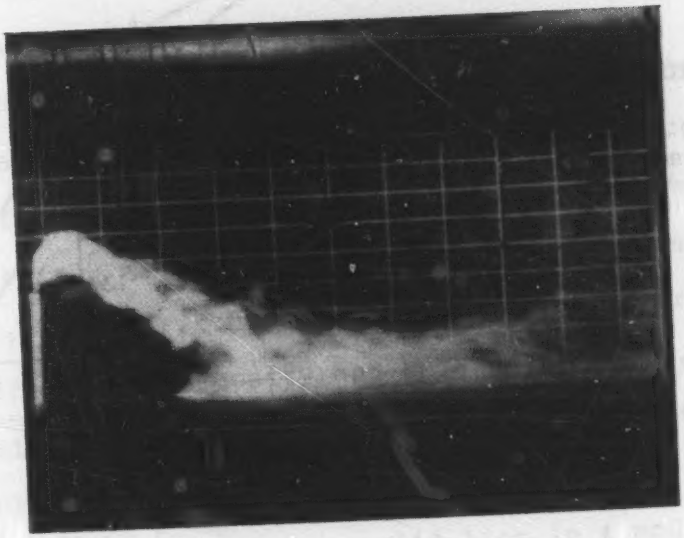

Figure 22. Side-view of a plume, which is very dense (about 4x air), bending downwind and earthward from its source stack (from Hoot et al, 1973).

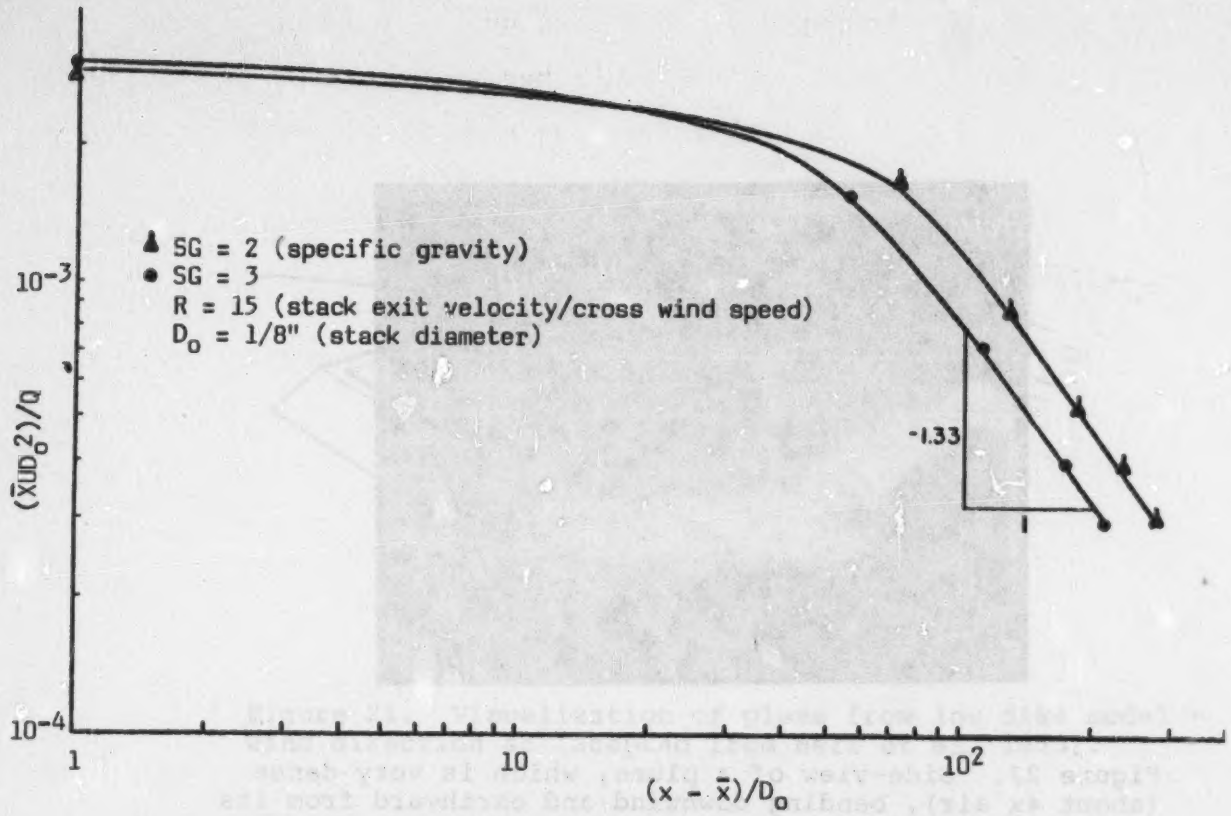

Figure 23. Maximum concentration vs downstream distance, plumes in a laminar crosswind, R = 15, D_o = 1/8 inch, $\bar{x}$ = horizontal distance to plume high point (adapted from Hoot et al, 1973).

Several tens of accident evaluation reports have been published related to large releases of hazardous gases from high pressure pipelines, railroad tankcars and tractor-trailer tankers. There is, however, only a small amount of information available regarding the meteorology, terrain, transport, and diffusion in each case. Some cases with relevant information are described, compared, and classified in Table 3. The common feature of interest here is the negative buoyancy of the released gas.

Part of the problem of describing the behavior of a heavy gas release is that of defining the turbulent mixing process across the air-gas interface. According to Csanady (1978) the turbulent mixing at a density interface may be such that the flow behaves much like a wall surface layer. However, the interface between different density fluids alters the effects of viscosity and roughness length. Figure 24 shows law of the wall* velocity profiles in air for a smooth solid wall and different hydrostatic stability conditions of the air. Figure 25 shows the smooth wall law plotted as a solid line in a modified height coordinate involving an effective viscosity. The data shown were taken by Wu (Csanady, 1978).

The experimental data in Figure 25 represent the speed profile across a turbulent density-interface layer. A simplified approach to

---

* The "law of the wall" is a term frequently used in fluid dynamics to describe the non-dimensional logarithmic relation for a universal velocity distribution of fluid flow adjacent to a solid surface or wall. For the coordinates referred to, u is the fluid velocity at a distance z from the surface, u_* is the friction velocity $u_* = \sqrt{\tau/\rho}$, τ is shearing stress, ρ is fluid density, and ν is kinematic viscosity. For the modified coordinates of Figure 25, ν is replaced by ν_e, an "effective viscosity." The data were taken by Wu (Csanady, 1978).

TABLE 3.

Observations from Accidental Releases of Heavy Gases into the Atmosphere

(Compiled from Eisenberg, Lynch and Breeding, 1975)

Case:
Flixborough, England
1 June 1975
time: unknown

Substance:
Cyclohexane (mol. weight = 84)

Containment Condition:
145°C, 120 psi
28-in-D. Pipe

Spill:
∿50-ton-spill, 50 ton min^{-1}
part flashed to vapor

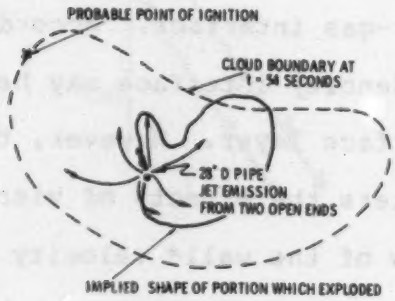
PROBABLE POINT OF IGNITION
CLOUD BOUNDARY AT t = 54 SECONDS
28" D PIPE
JET EMISSION FROM TWO OPEN ENDS
IMPLIED SHAPE OF PORTION WHICH EXPLODED

Cloud:
15-30 tons white vapor-mist in 54 s
∿50 m vertically thick
∿200 m diameter

Meteorology:
$\overline{U}$ = 9 ms^{-1}
ϕ = Southwest or ∿225°
Stability: unknown

Terrain:
Level.
Filled with chemical plant towers,
piping and buildings
(Industrial complex)

Ignition pt:
down-crosswind left edge of gas volume

Explosion pt:
1. down-crosswind left edge of exploded cloud
2. mid-crosswind left side of exploded cloud

TABLE 3. (cont.)

Case:
Franklin County, Missouri
9 December 1970
time: 10:20 p.m.

Substance:
Propane

Containment Condition:
8-inch pipeline
T (ambient), P >> atmospheric

Spill:
2-m-long split in underside of pipe
Geyser (out of 4 ft. deep, 10 ft. diameter crater) to a height of 15-20 m, 30,000 gallons in 24 minutes

Cloud:
Heavy white fog flowed downhill (to SW?) and slowly filled a shallow valley (about 300 m away?)
In 24 minutes valley was filled as far as 500 m from the rupture. Vapor volume about $3 \times 10^{+4}$ m^3. Flammable mixture covered area of about 4×10^4 m^2; it ignited and detonated. One fire branch going 300 m to Southeast in stream cut. A fireball followed which rolled E → W across valley bottom.

Meteorology:
$\bar{U} = 2.5$ ms^{-1}
ϕ = Northeast or 045^o
$T = 34^oF$
Stability: very stable atmosphere

Terrain:
Complex hill-valley-ridge with relief of around 30 m. Main valley ~1000 m wide

Ignition pt:
Running down to SE near leading SW or downwind edge of cloud in bottom of valley.

Explosion pt:
Near left downwind edge of cloud.

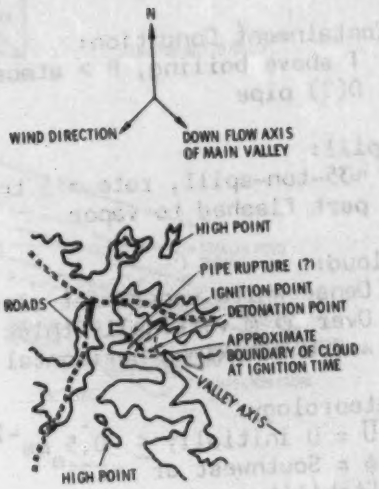

TABLE 3. (cont.)

Case:
Pensacola, Florida
11 September 1971
time: unknown

Substance:
Cyclohexane

Containment Condition:
T above boiling, P > atmospheric
D(?) pipe

Spill:
∿35-ton-spill, rate = 1 ton min^{-1}
part flashed to vapor

Cloud:
Dense white vapor-mist cloud (40 tons)
Over 35 m vertically thick
~ 700 m maximum horizontal dimension

Meteorology:
$\bar{U}$ = 0 initially $\leq$ 0.5 ms^{-1}
ϕ = Southwest or ∿225°
Stability: unknown

Terrain:
Level.
Large industrial complex all around..

Ignition pt:
Cloud did not ignite
Cloud entered furnace and therein
produced black smoke.
Cloud dissipated in unknown manner.

Explosion pt:
No explosion even with confinement and
contact with flame.

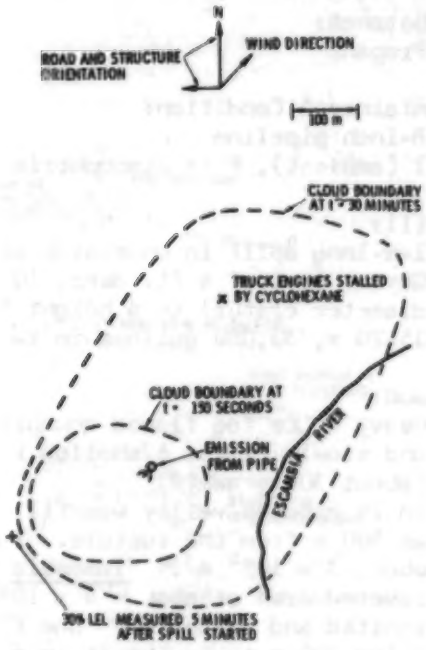

TABLE 3. (cont.)

Case:
Austin, Texas
22 February 1973
time: 10:53 p.m.

Substance:
NGL (natural gas liquids - not to be confused with liquified natural gas)

Containment Condition:
10-inch pipeline,
T(ambient); P = 525 psig

Spill:
300,000 gallons spewed onto ground and air, flowed into ditches and road between them
Continuous spill

Cloud:
White fog over ditches, road, embankment down to road from pipeline
Depth of fog: ∿1 meter
Length of fog: ∿800 meter
Concentrated enough to stall car engines near both ends of cloud
However, engine nearly restarted at cloud ignition point

Meteorology:
$\bar{U}$ = 3 ms^{-1} at t = 10:53, = 0 at t = 11:30 p.m.
ϕ = Southeast, E
Stability: unknown Cloudy
T = 44°F
r.h. = 86 %

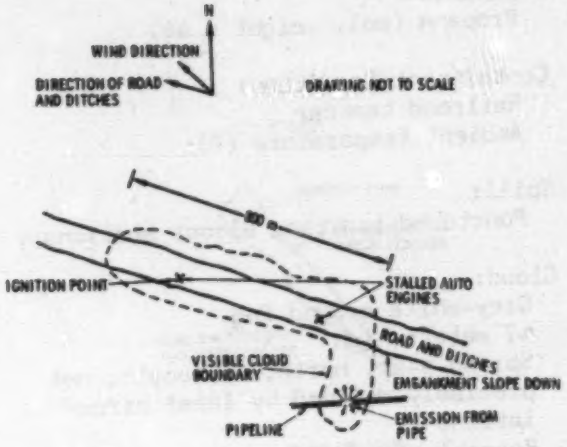

TABLE 3. (cont.)

Case:
Decatur, Illinois
19 July 1974
time: 5:30 a.m.

Substance:
Propane (mol. weight = 44)

Containment Condition:
Railroad tankcar
Ambient temperature (?)

Spill:
Punctured tankcar, almost stationary

Cloud:
Grey-white ground fog.
∿7 meters high
Spread east, north, and south; not precisely defined by local circulations
Possibly patchy due to terrain and wind.

Meteorology:
$\overline{U}$ = 5 ms^{-1}
ϕ = 020^{o}
T = 77^{o}F
Td = 68^{o}F
Stability: stable (inferred from blast wave refraction)

Terrain:
Very gentle rolling.
Town and railyard.
Decatur lake 1 km away
long shallow depression.

Ignition pt:
Several within 10 minutes.
Unspecified location relative to cloud.

Explosion pt:
Pockets of explosion within 10 minutes.

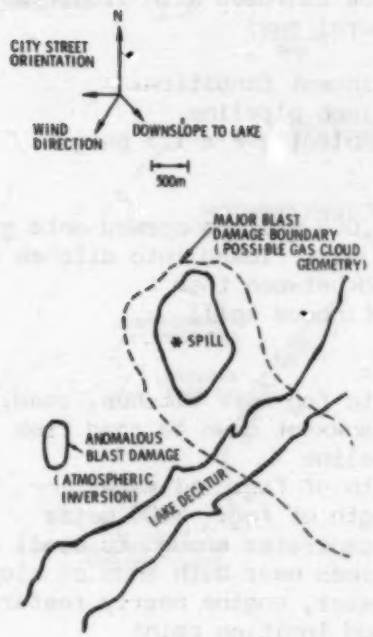

TABLE 3. (cont.)

Case:
E. St. Louis, Illinois
22 January 1972
time: 6:20 a.m.

Substance:
LPG (propylene and propane)
(mol. weights 42 and 44)

Containment Condition:
Railroad tankcar
T atmospheric, P > atmospheric

Spill:
30,000 gallons spewed along a line ~400 m long at 7 ms^{-1} or over a time interval of 60 s vaporized.

Cloud:
Visible cloud
~70 m wide x 400 m long
drifted along direction of railroad tracks
Not nearly stoichiometrically mixed
1st flaming traveled horizontally
2nd flaming traveled upward
3rd cycle was a large fireball explosion followed by a more severe explosion

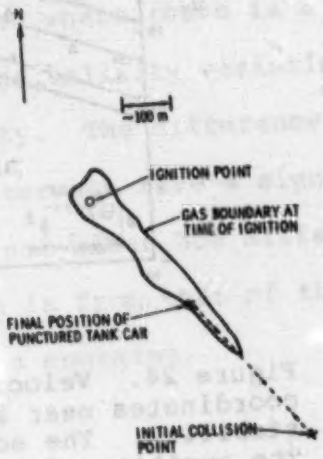

Meteorology:
$\bar{U}$ = 7 ms^{-1}
ϕ = unknown
Stability: unknown, most likely slightly stable-to-neutral

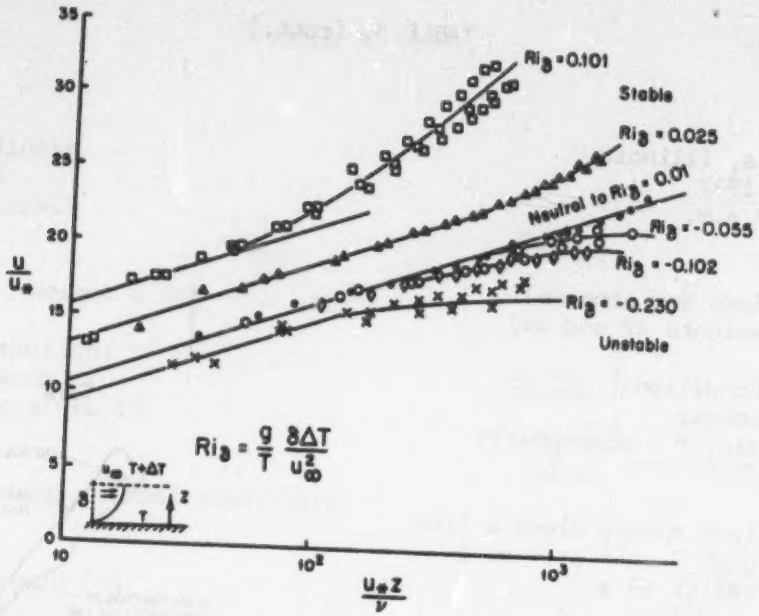

Figure 24. Velocity profiles in law of the wall coordinates near a smooth solid wall for varying stability. The scale of the abscissa is logarithmic. The position of the logarithmic line is displaced upward under stable conditions and downward under unstable conditions. Stability is characterized by a bulk boundary layer Richardson number, as illustrated (from Csanady, 1978).

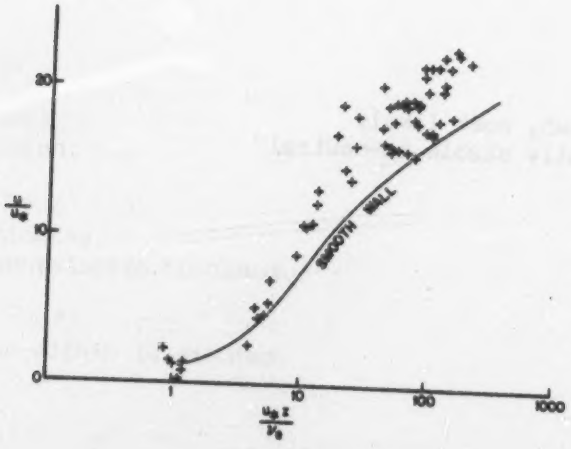

Figure 25. Experimental data of Wu in modified law of the wall coordinates (from Csanady, 1978).

modeling of transport and diffusion of dense gas for channeled flow may be derived from this type of result.

Another complicating feature of the hazardous gas spill problem is that it may involve double diffusion with diffusion of both mass and heat independently. Analogous double diffusive processes described by Turner (1978) occur in the ocean, for example, where there is a systematic association between temperature and salinity variations such that they have opposing effects on the density. The differences in molecular diffusivity of heat and salt in water can have a significant effect on mixing. On the other hand, it is not clear how different the turbulent transport of a heavy gas substance is from that of the turbulent transport of the heat which the gas contains.

2.5 In the Lee of Obstacles to Flow

Two considerations within the general category of flow and mixing near buildings seem relevant to the problem of effects on nuclear power plants of hazardous gas releases:

(1) The early shape and volume of the gas-air cloud

(2) The transport and diffusion enhancement or constraint caused by nearby buildings or structures

Gifford (1976) noted that little is known about the properties of diffusion in wakes. Further, because of wakes, very few sources of atmospheric contaminant gas or aerosol retain even approximately the point source character assumed in much of diffusion theory. The wake contains both fine scale and obstacle size turbulence. Usually a significant flow cavity exists in the near lee space where a

contaminant may recirculate. A smaller cavity also may exist on the upwind side. Cavity observations will be cited in a later paragraph.

Wind tunnel observations by Halitsky (1968) suggest that a wake an obstacle affects plume diffusion such that a first approximation t the ground-level downwind centerline concentration may be made using the following formula by Gifford (1976):

$$X/Q = ((\pi\sigma_y\sigma_z + CA)\bar{u})^{-1}$$

where

A = area of cross section of obstacle normal to the mean wind direction

C = the fraction of A over which the plume is initially dispersed

Halitsky found $C \cong 1/2$ to be appropriate.

Barry (1964) summarized atmospheric and wind-tunnel tests and al found that $C \cong 1/2$. Gifford (1976) described two defects to this simple diffusion model for a plume released in a wake:

Defect 1 - The model does not account for significant meandering of the atmospheric wind affecting wake diffusion in low wind speed conditions with stable stratification. This has been verified by Halitsky and Woodard (1974).

Defect 2 - The model does not incorporate a reduced diffusion rate for a steady direction of wind.

Wind tunnel plume tests by Symes and Meroney (1970) and Meroney and Yang (1971) indicate that, for stability categories B, C, and D,

$$X/Q \propto x^{-0.6 \text{ to } -1.0}$$

while field observations indicate that

$$X/Q \propto x^{-1.5}$$

Thus, underestimation of concentration is a possibility.

Abbey (1976) summarized experimental results on concentrations downwind of buildings as follows:

(1) Effluent released in the leeward cavity is trapped and becomes well mixed.

(2) Locating the release near the ground in the cavity strongly affects rooftop concentrations. The amount of scatter in the data and a comparison with Pasquill typing scheme predictions are shown in Figure 26. The conditions of release and sampling, and building configuration and size, vary in the experimental results plotted on these graphs.

(3) When the wind flow is diagonal across a square-plan building the wake eddies extend beyond the crosswind width of the building.

Dickson, Start and Markee (1969) measured the aerodynamic effects of the EBR-II reactor complex on the concentration of a contaminant released 1 m above the ground at the downwind edge of the containment building. Sampling was also done at 1 m above the ground. Graphs of maximum concentration as a function of downwind distance for lapse and for inversion conditions are shown in Figures 27 and 28 which indicate an exponential decrease of between

$$X \propto x^{-1} \text{ and } x^{-1.5}$$

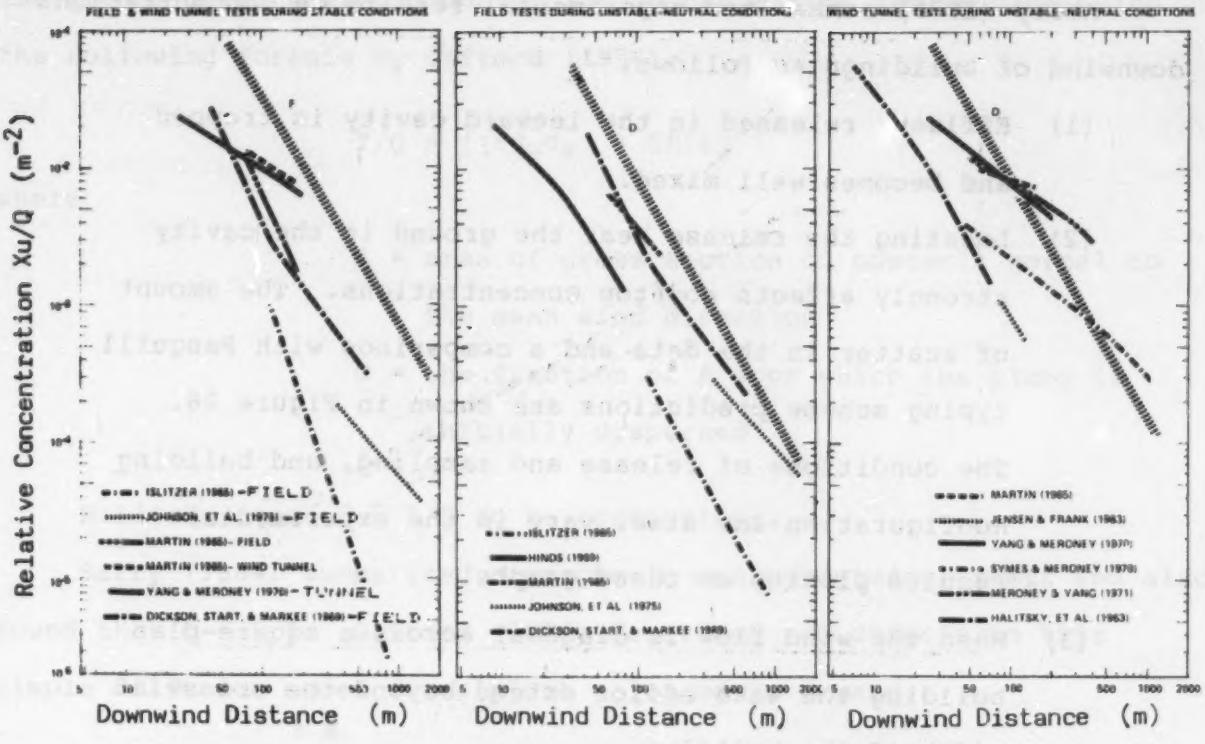
FIELD & WIND TUNNEL TESTS DURING STABLE CONDITIONS
FIELD TESTS DURING UNSTABLE-NEUTRAL CONDITIONS
WIND TUNNEL TESTS DURING UNSTABLE-NEUTRAL CONDITIONS
Relative Concentration Xu/Q (m⁻²)
ISLITZER (1966) - FIELD
JOHNSON, ET AL. (1975) - FIELD
MARTIN (1965) - FIELD
MARTIN (1965) - WIND TUNNEL
YANG & MERONEY (1970) - TUNNEL
DICKSON, START, & MARKEE (1969) - FIELD
ISLITZER (1965)
HINDS (1969)
MARTIN (1965)
JOHNSON, ET AL. (1975)
DICKSON, START, & MARKEE (1969)
MARTIN (1965)
JENSEN & FRANK (1963)
YANG & MERONEY (1970)
SYMES & MERONEY (1970)
MERONEY & YANG (1971)
HALITSKY, ET AL. (1963)
Downwind Distance (m)
Downwind Distance (m)
Downwind Distance (m)

Figure 26. Relative concentrations normalized by windspeed as a function of distance for (a) field and wind tunnel tests during stable conditions, (b) field tests during unstable-neutral conditons, and (c) wind tunnel tests during unstable-neutral conditons. Pasquill F and D curves are shown for comparison (adapted from Abbey, 1976).

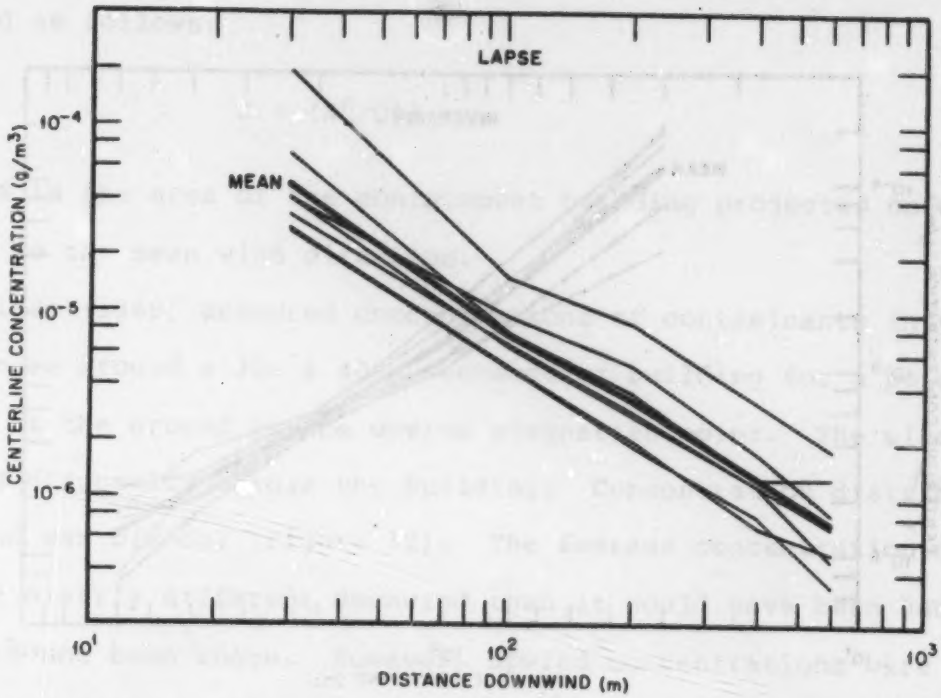

Figure 27. Centerline concentration vs downwind distance for lapse conditions (from Dickson et al, 1969).

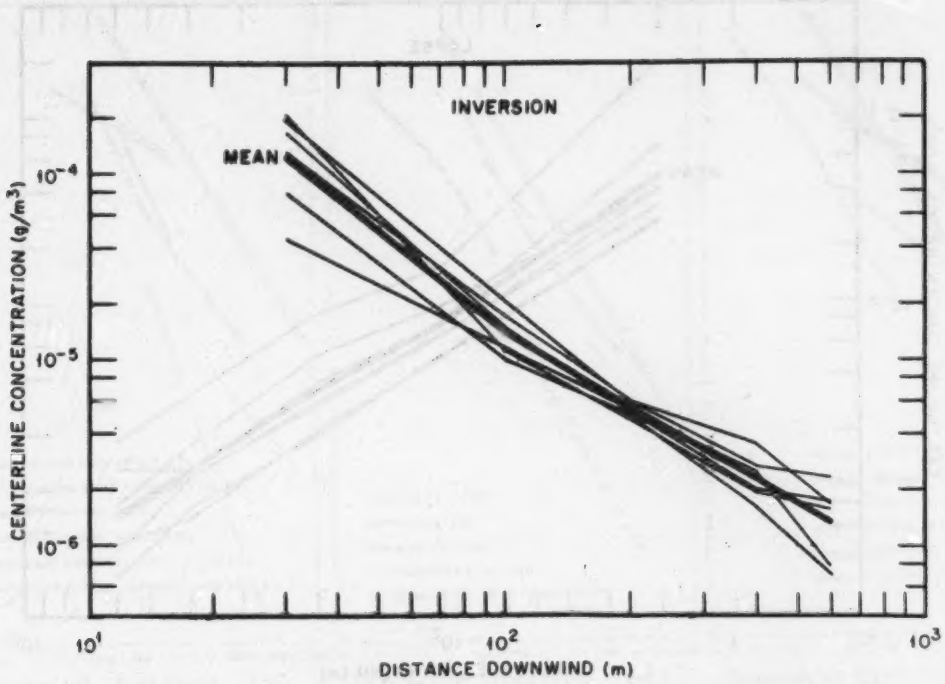

Figure 28. Centerline concentrations vs downwind distance for inversion conditions (from Dickson et al, 1969).

Measured concentration results from two test cases for inversion conditions are shown in Figures 29 and 30 in K-units defined below.

Figure 31 shows a scaled wind tunnel test result for the same geometry as above but with lower wind speed and neutral atmospheric stratification. Concentration contours are for K-values which are defined as follows:

$$K = (X\bar{u}/Q)A$$

where A is the area of the containment building projected on a plane normal to the mean wind direction.

Hinds (1969) measured concentrations of contaminants in the atmosphere around a 30- x 40-m rectangular building for a point source placed at the ground at the upwind stagnation point. The wind was blowing diagonally across the building. Concentration distribution downwind was bimodal (Figure 32). The average concentration maximum was not clearly different downwind than it would have been had the building not been there. However, upwind concentrations were greater than without the building, certainly because of the reduced entrainment where the plume is in contact with the walls of the building.

Start et al (1977) measured the wake effect on atmospheric diffusion of tracer material in the vicinity of the large power plant complex at Rancho Seco. Figure 33 is a topographic map of the site. The complex is about 400 m in diameter and the two cooling towers rise about 150 m above plant grade. The near-field airflow is a complex

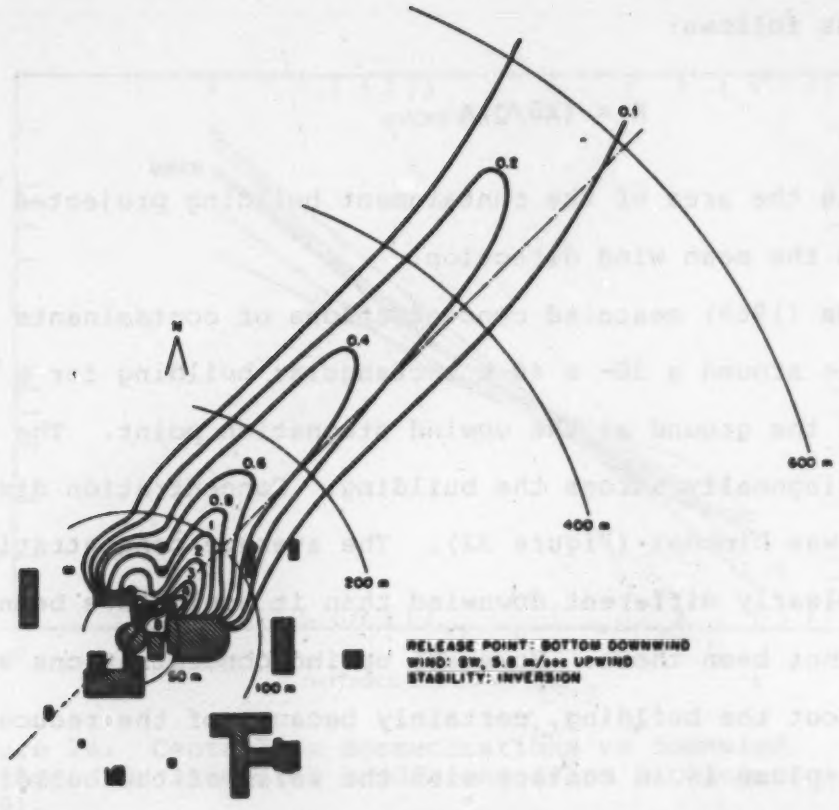

Figure 29. K-mean isopleths of effluent released from containment building during inversion conditions (from Dickson et al, 1969).

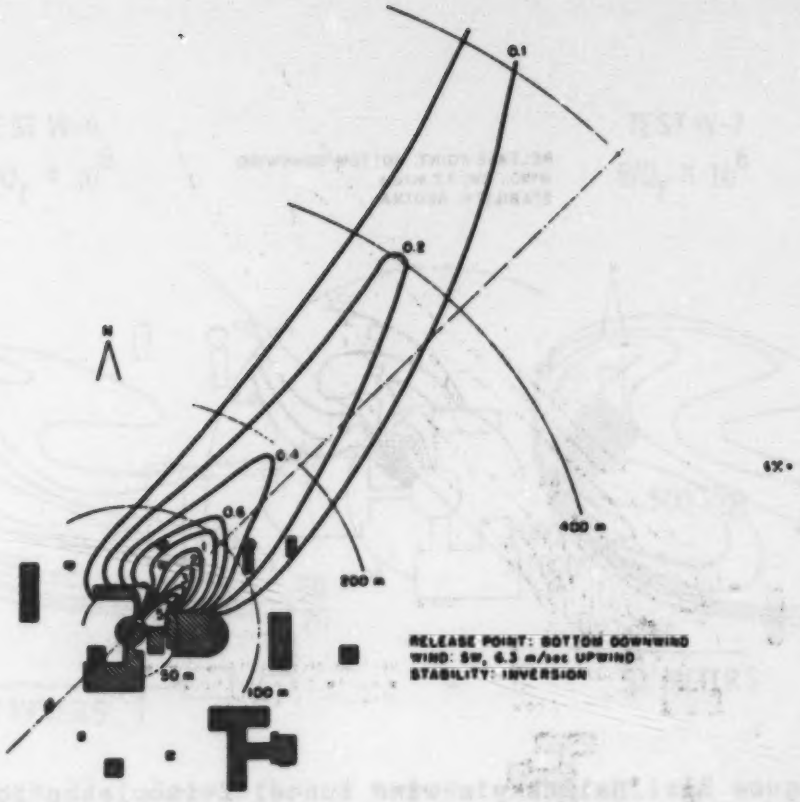

Figure 30. K-maximum isopleths of effluent released from containment building during inversion conditions (from Dickson et al, 1969).

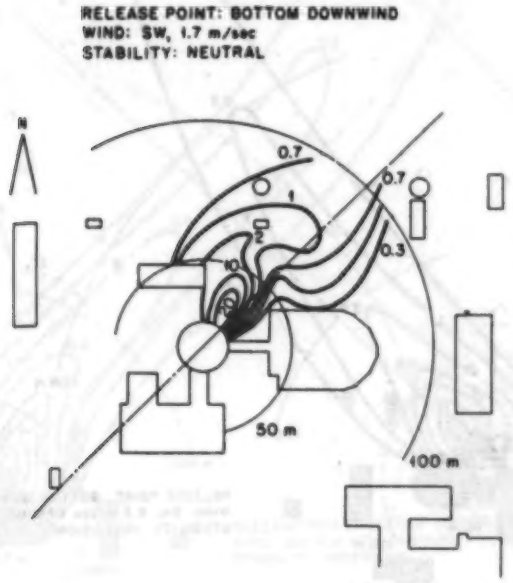

Figure 31. Halitsky's wind tunnel K-isopleths for neutral release (from Dickson et al, 1969).

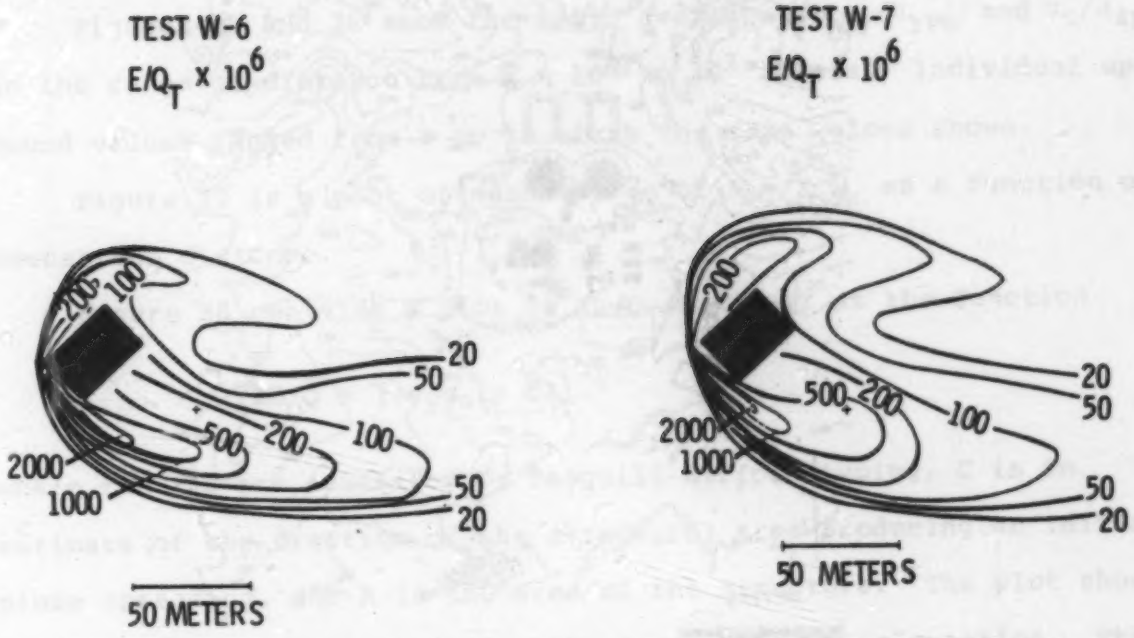

Figure 32. Isopleths of exposure (normalized to source strength) for the test series, with position of the self-orienting-real-time-sampler (SORTS) indicated by + (adapted from Hinds, 1969).

Figure 33. Topography of the Rancho Seco study site, showing the details of terrain that influenced the measured concentrations. Heights are feet above sea level (from Start et al, 1977).

result of wakes, cavities and channels interacting with buildings. Figure 34 shows the source and sampler locations (numbered). The wind speeds were 1 to 3 m/s and $\sigma_\theta \leq 20^o$. The average concentrations were much less than predicted by Pasquill-Gifford methods; that is, measured σ_y and σ_z values were much larger than those inferred from σ_θ measurements.

Figures 35 and 36 show the ratio averages of σ_y/σ_{yPG} and σ_z/σ_{zPG} in the range of distance from $x = 10^2$ to 10^3 meters. Individual upper bound values ranged from 3 to 10 times the mean values shown.

Figure 37 is a plot of mean values of X_{PG}/X_{max} as a function of downstream distance.

Figure 38 contains a plot of Xu/Q (maximum) as the function

$$X\bar{u}/Q = (\pi\sigma_y\sigma_z + CA)^{-1}$$

where the σs are estimated by Pasquill-Gifford typing, C is an estimate of the fraction of the structural area producing an initial plume spreading, and A is the area of the structure. The plot shows that the CA area term dominates the concentration calculation. The expression appears to be fundamentally correct.

Figure 39 shows the normalized concentration isopleths for a surface release at the containment structure under NRC stability category G (U.S. N.R.C. Reg. Guide 1.23). It should be kept in mind that the source diameter is small compared to the containment diameter. Figure 40 shows the change in concentration pattern when the release is from roof height under the same NRC stability category G. The other two maps, Figures 41 and 42, show the results for ground- and

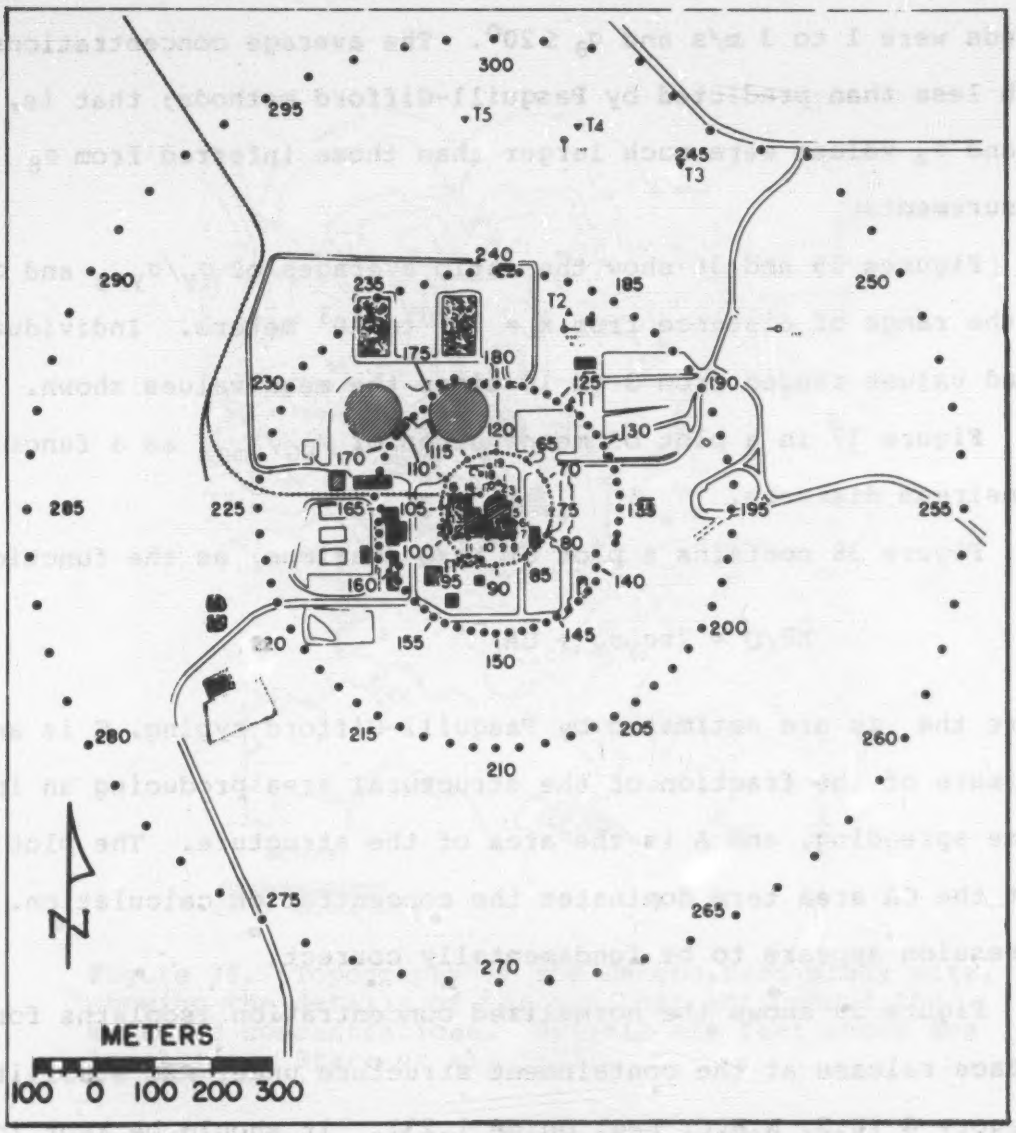

Figure 34. Plotplan of Rancho Seco study site, indicating sampler positions (from Start et al, 1977).

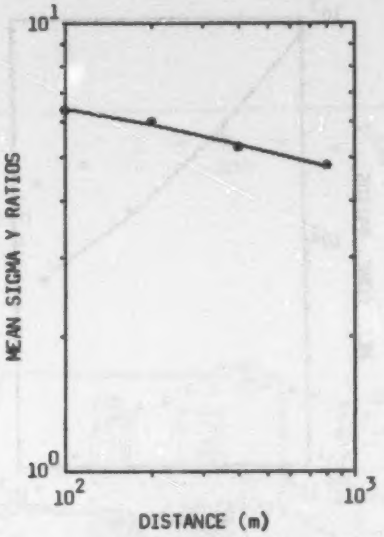

Figure 35. Mean ratios for calculated (observed) sigma-y values divided by expected Pasquill-Gifford values. * denotes the mean ratios for each distance. The line is a regression fit of the mean values (adapted from Start et al, 1977).

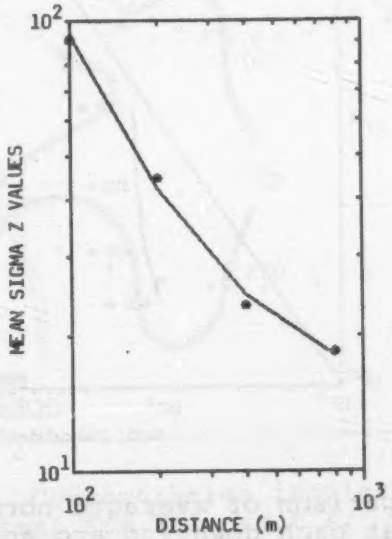

Figure 36. Mean ratios for calculated (observed) sigma-z values divided by expected Pasquill-Gifford values (adapted from Start et al, 1977).

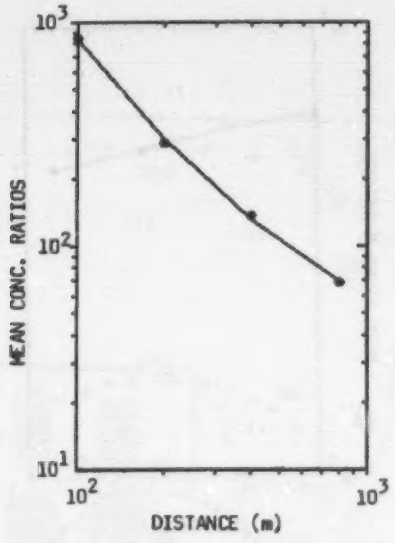

Figure 37. Mean ratios for Pasquill-Gifford values divided by observed maximum concentration values (adapted from Start et al, 1977).

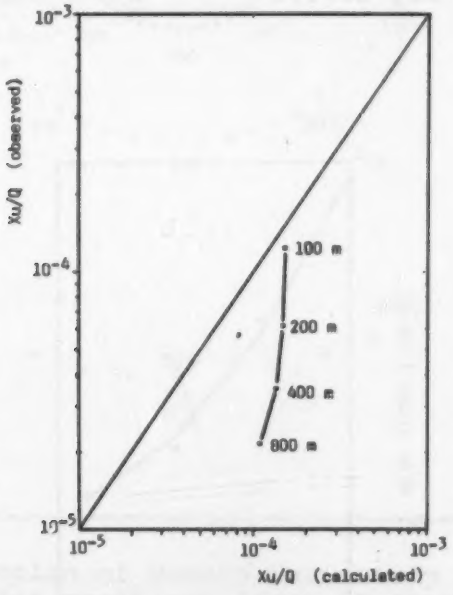

Figure 38. Comparison of averaged normalized maximum concentrations at each downwind arc and calculated normalized peak concentrations. Calculated values use Pasquill-Gifford sigma values plus an added term to incorporate an effect due to building cross sectional area for stabilities D - F (adapted from Start et al, 1977).

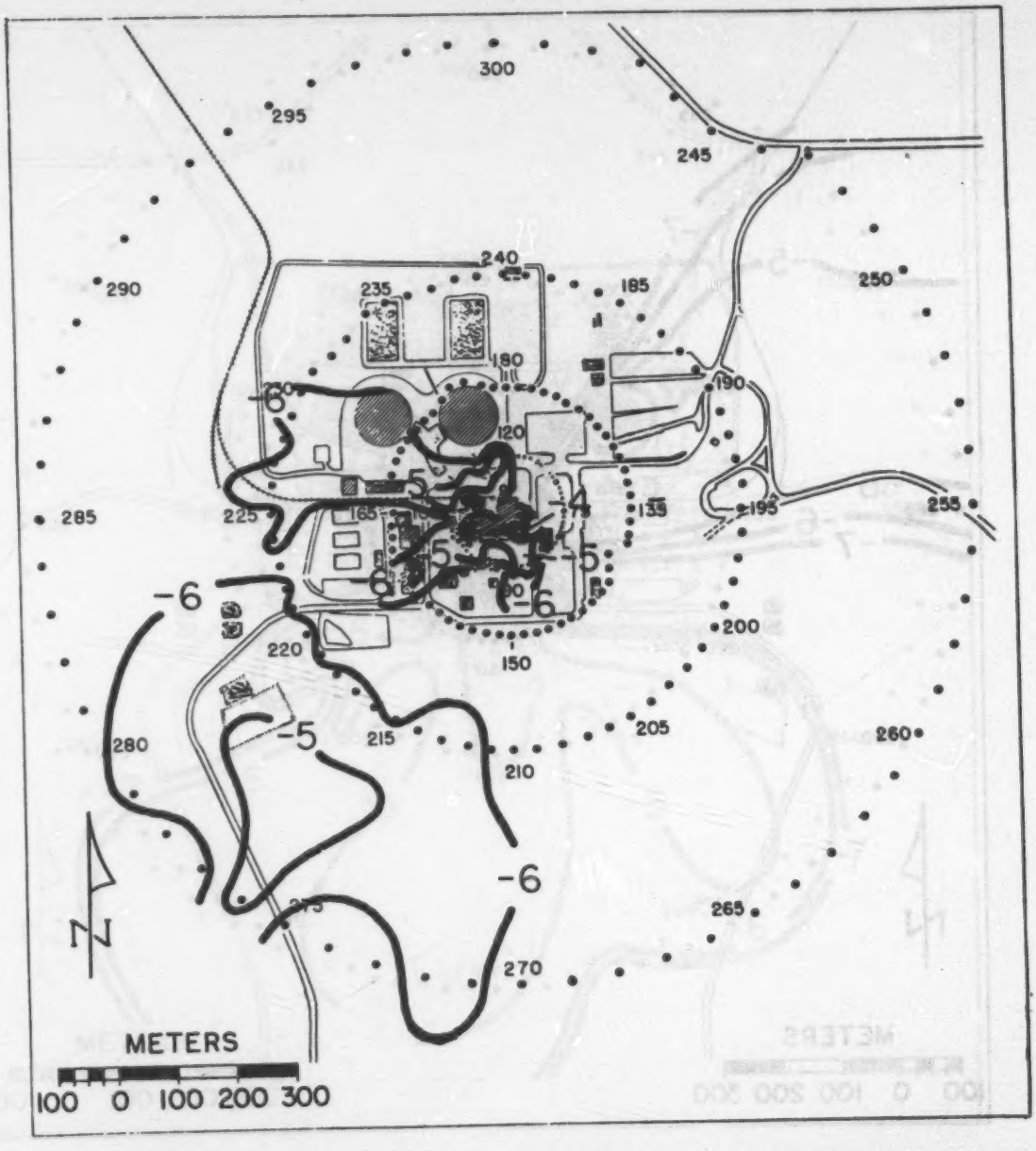

Figure 39. Concentration isopleths ($X\bar{u}/Q$ in negative powers of ten) for F12, test 4. Tracer was released from surface positions G5 under NRC stability category G. Mean tower wind at release height was from 038 degrees at 1.3 m/s (from Start et al, 1977).

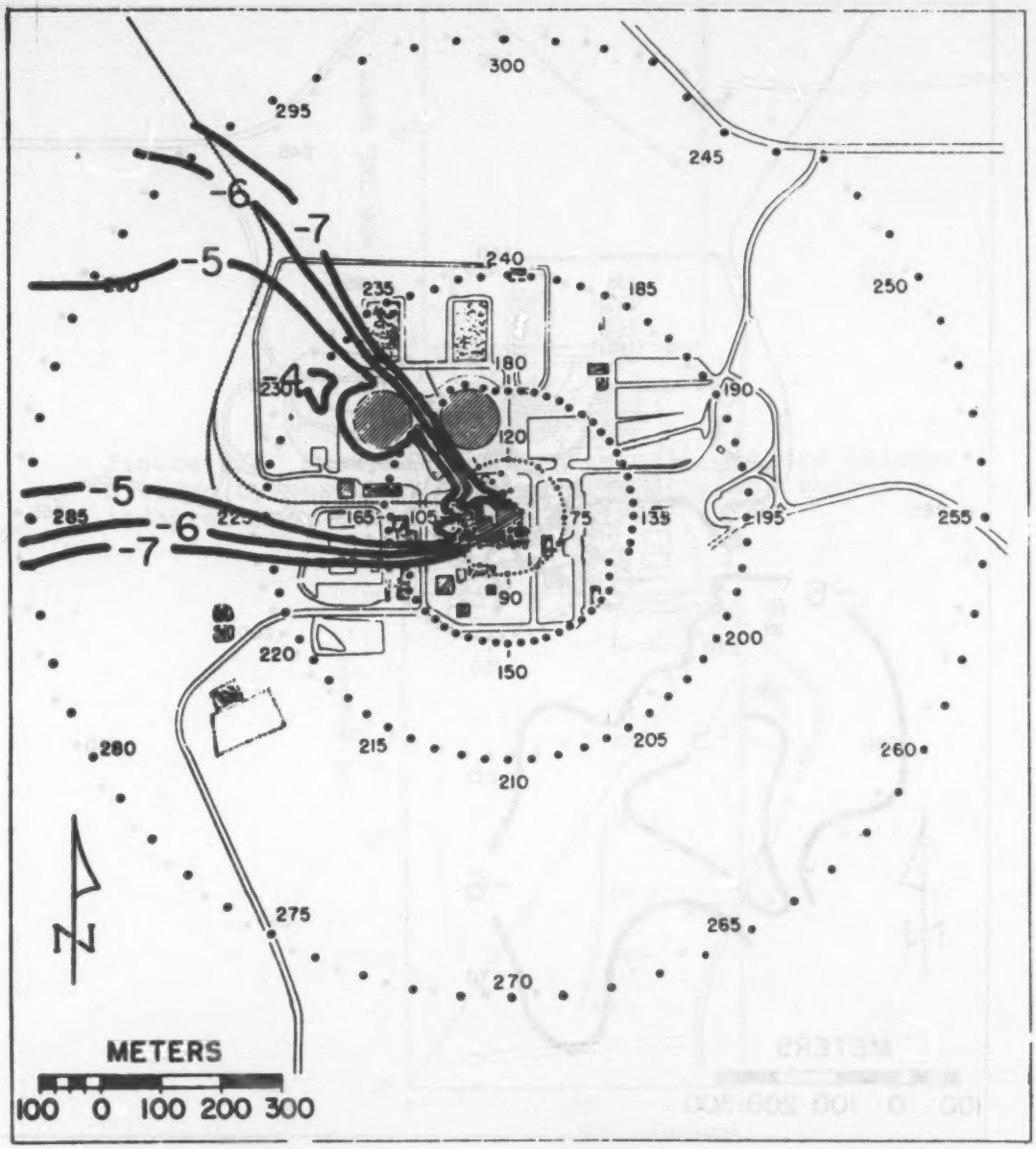

Figure 40. Concentration isopleths ($X\bar{u}/Q$ in negative powers of ten) for SF6, test 8. Tracer was released at auxiliary building roof under NRC stability category G. Mean tower wind at release height was from 110 degrees at 2.5 m/s (from Start et al, 1977).

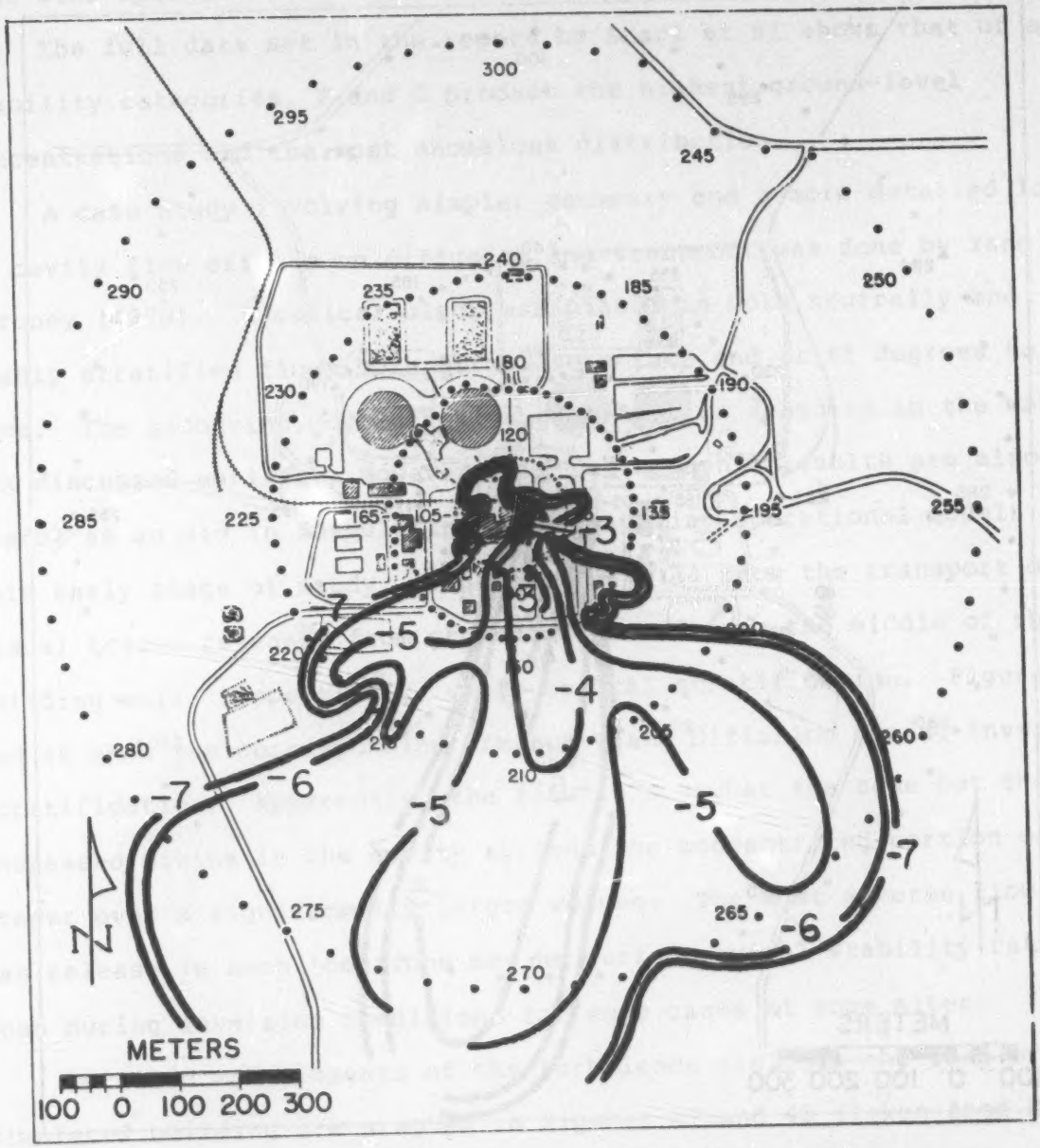

Figure 41. Concentration isopleths ($X\bar{u}/Q$ in negative powers of ten) for F12, test 10. Tracer was released at surface position G5 under NRC stability category F. Mean tower wind at release height was from 330 degrees at 3.0 m/s (from Start et al, 1977).

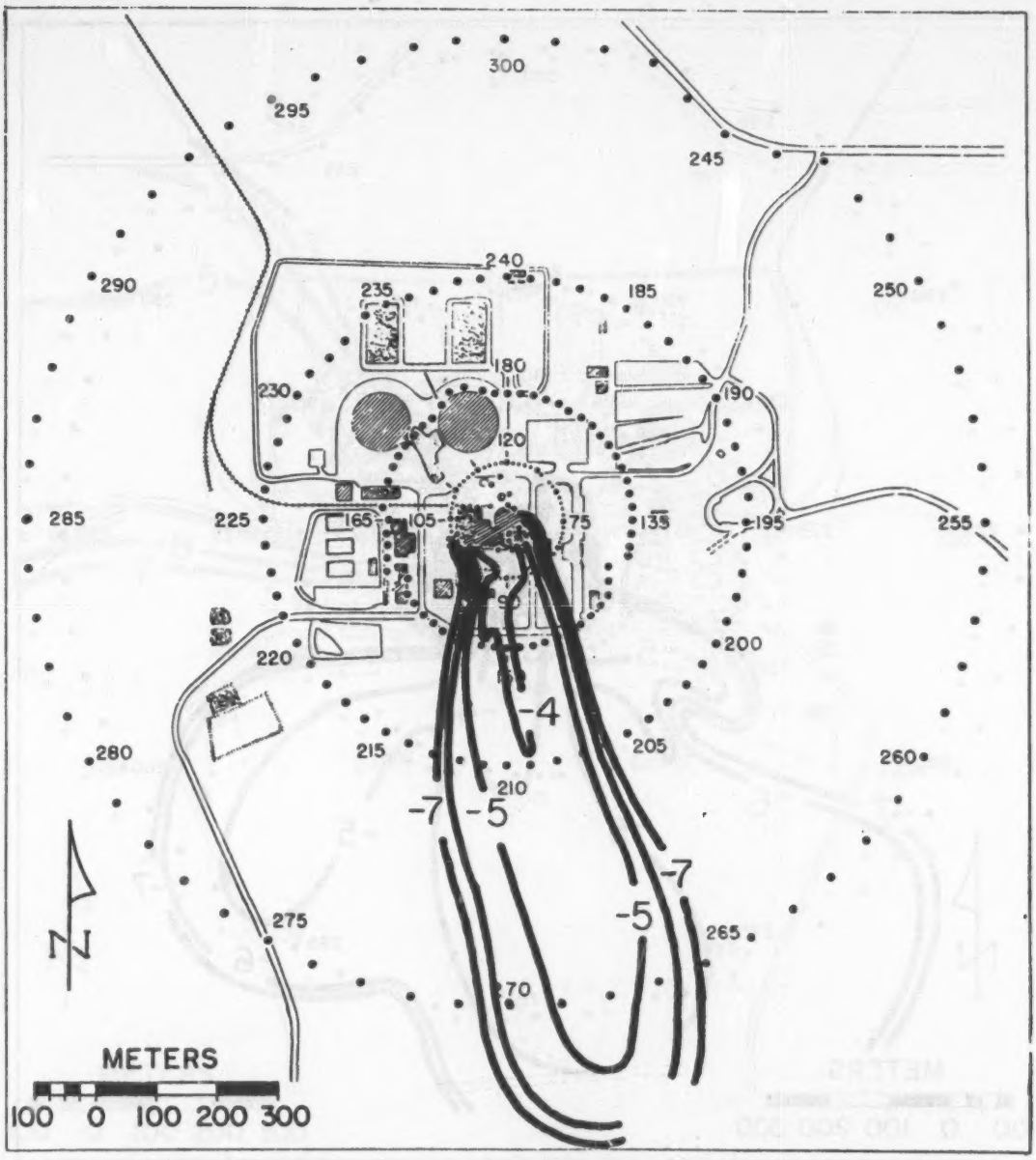

Figure 42. Concentration isopleths ($X\bar{u}/Q$ in negative powers of ten) for SF6, test 10. Tracer was released at auxiliary building roof under NRC stability category F. Mean tower wind at release height was from 346 degrees at 4.9 m/s (from Start et al, 1977).

roof-level releases under NRC stability category F. Note, however, that wind speeds increase from 1.3 to 4.9 m/s from Figure 39 to Figure 42. The full data set in the report by Start et al shows that of all stability categories, F and G produce the highest ground-level concentrations and the most anomalous distribution.

A case study involving simpler geometry and a more detailed look at cavity flow effects on diffusion and transport was done by Yang and Meroney (1970). A cubical block was placed in both neutrally and stably stratified flows both normal to a face and at 45 degrees to a face. The alongwind concentration distribution measured in the wake was discussed earlier. However, the photographic results are also useful as an aid in formulating and evaluating operational models at this early stage of study. Figures 43 and 44 show the transport of visual tracer released from ground level and from the middle of the building wall, respectively, under neutral stratification. Figures 45 and 46 show the corresponding transport and diffusion during inversion stratification. Apparently, the flow is somewhat the same but the increased mixing in the cavity spreads the concentrated portion of tracer over a significantly larger volume. The most adverse flow for a gas release in such locations may be during neutral stability rather than during inversion conditions for some cases at some sites.

Detailed measurements of the turbulence field in the wake of a simulated building are graphed in Figures 47 and 48 (taken from Hansen, Peterka and Cermak, 1974). The increase in rms longitudinal turbulence caused by the building wake divided by mean local longitudinal wind speed is shown. In Figure 47 the data for about rooftop height

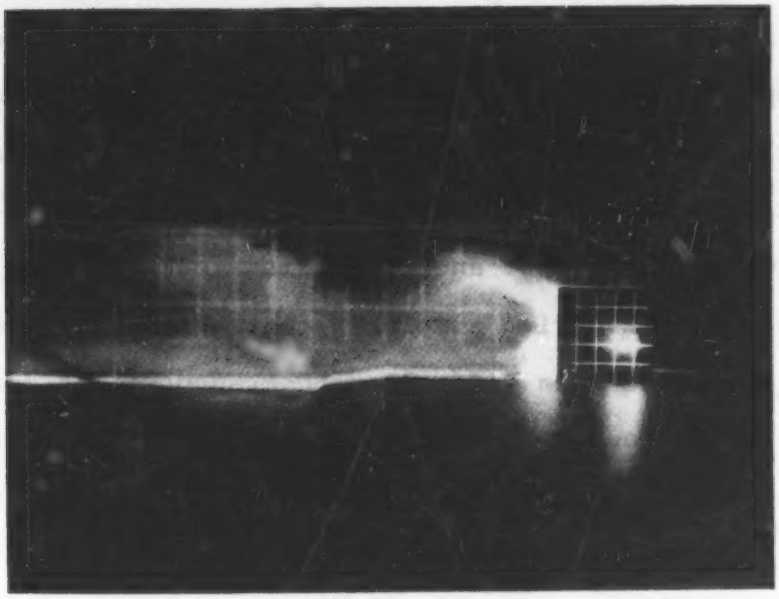

Figure 43. $\theta = 0^{o}$, bottom exit port, neutral stratification (from Yang and Meroney, 1970).

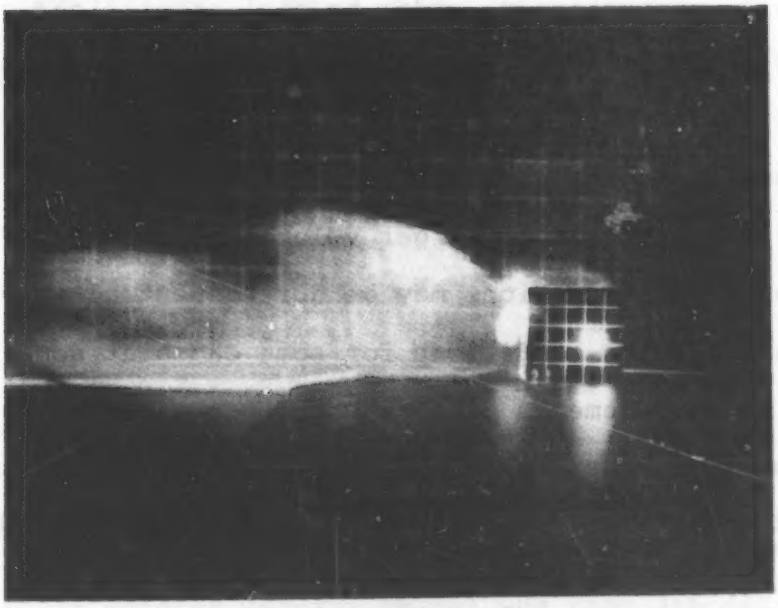

Figure 44. $\theta = 0^{o}$, middle exit port, neutral stratification (from Yang and Meroney, 1970).

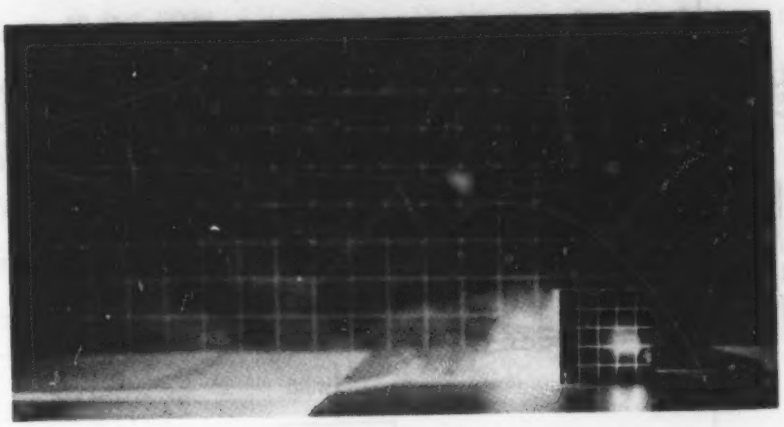

Figure 45. $\theta = 0^{o}$, bottom exit port, inversion stratification (from Yang and Meroney, 1970).

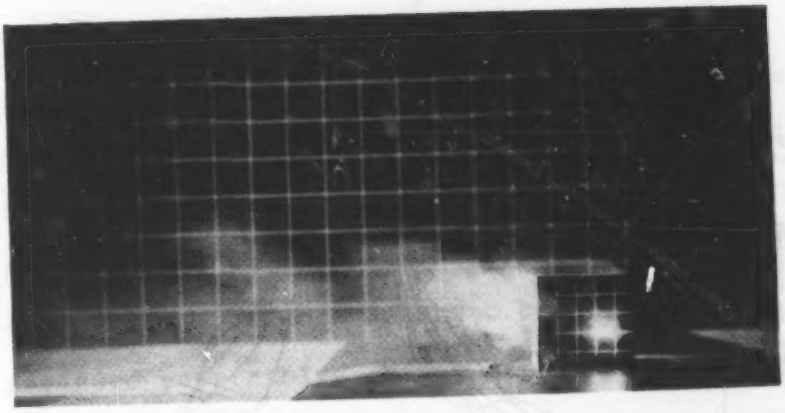

Figure 46. $\theta = 0^{o}$, middle exit port, inversion stratification (from Yang and Meroney, 1970).

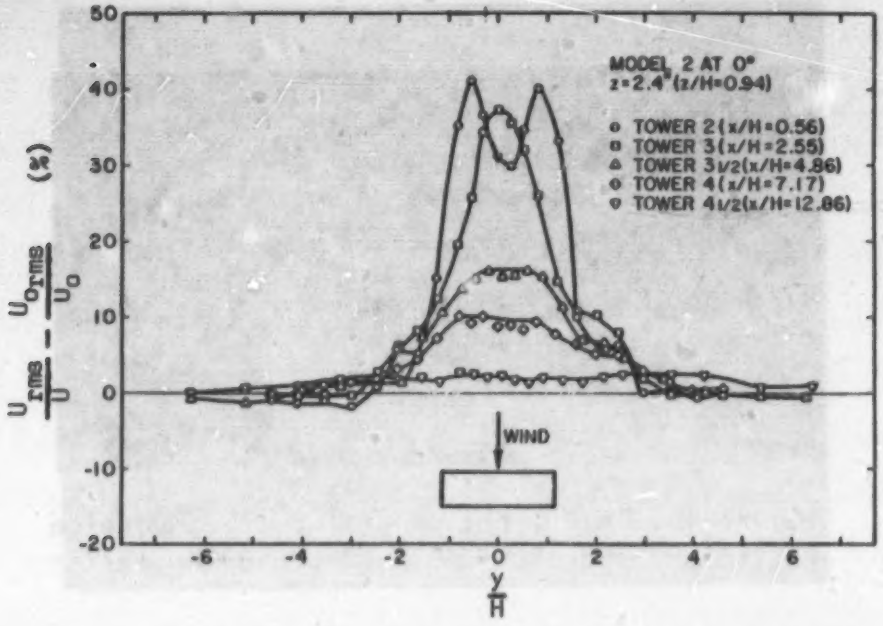

Figure 47. Lateral profiles of turbulence intensity excess in the wake of the building at 0 degrees (adapted from Hansen et al, 1974).

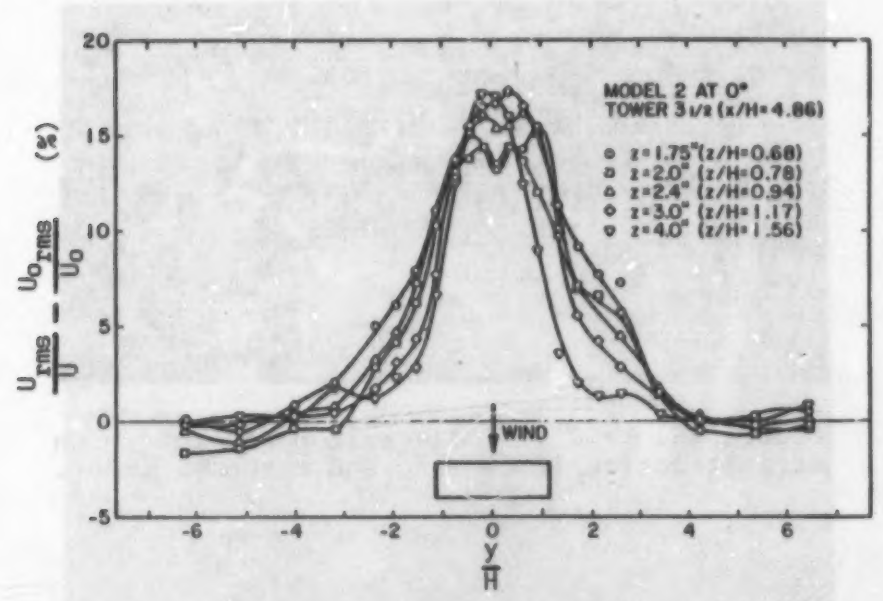

Figure 48. Lateral profiles of turbulence intensity excess in five heights above the ground on tower 3-1/2 (adapted from Hansen et al, 1974).

(Z/H = 0.94) are shown at five distances from the downwind edge of the building, X/H = 0.6, 2.6, 4.9, 7.2 and 12.9. Thus mixing capability in the cavity and the rest of the wake is measured. Beyond the cavity, at X/H = 4.9, the turbulence intensity added by the building wake varies only slightly with height up to Z/H = 1.6 (Figure 48). Data from the cavity region itself are difficult to obtain in a wind tunnel because of flow reversal problems and the small size of the models studied.

2.6 On or Near Highways

Gifford (1976) noted that an important special aspect of diffusion near highways is the presence of wakes generated by vehicles. However, the response of drivers to a major hazardous gas accident would be difficult to predict. Thus, some simplified treatment will probably have to be developed. It is not considered further here.

2.7 Irregular and Rugged Terrain

Irregular and rugged terrain can dominate the airflow and diffusion for all distances from a source, for all stability categories, and for all wind speed regimes. Terrain effects are implicitly included in the observations reported in other subsections of this report. While much work needs to be done on this problem, it will not be reviewed separately. Major experimental and modeling programs are presently underway to further elucidate complex terrain effects (Barr et al, 1977).

2.8 Over Cities

This subclass, further complicated by heat island effects, is in somewhat the same state as that for irregular and rugged terrain and

also will not be separately reviewed.

2.9 Very Close to the Source

A short distance is defined as a distance, x, from the source, whose diameter, D, is such that $x/D < N$, where N is of the order of 20. Many of the observations cited above fall in this category. Some work was done by Hardee and Lee (1975) on details of initial dilution of flammable gas releases. They presented a 3-stage description of gas release from a tank rupture which may be useful for certain situations.

SECTION 3.0 Models of Flow and Diffusion of Dense Gas in the Atmospheric Boundary Layer

3.1 Properties of Gasflows Which are to be Modeled

Table 4 shows property data for representative gases of concern which are useful in estimating buoyancy effects. As can be seen, chlorine is significantly more dense than air while methane is more dense immediately following a rapid release from conditions of stored pressure and temperature. Ammonia and methane at STP are much lighter than air. Of course, as any gas of a differing density becomes well mixed with ambient air, properties of the mixture approach those of air.

TABLE 4

Some Comparative Properties of Air, Ammonia, Chlorine, and Methane

Gas	Molecular Weight	Condition	Density g/l	Boiling Point °C	Density Ratio to Air
Air	29	STP	1.29		1.0
NH_3	17	STP	0.76	-33.4	0.59
Cl_2	71	STP	3.2	-34.6	2.5
CH_4	16	STP	0.72	-164	0.55
"		-50°C	0.88		0.68
"		-100°C	1.13		0.87
"		-164°C	1.79		1.39

A model, or set of submodels, which represents the wide range of properties possible for methane will also span the buoyant properties of Cl_2 and NH_3. There will be some differences in chemical effects,

such as interaction with water droplets and possibly some significant radiation effects. The changes in molecular state which may occur are another complicating factor.

3.2 Recommended Interim Models

The observations and reviews cited in Section 2 show that there is only a limited physical basis for applying or judging typing schemes and theoretical diffusion models such as those of Pasquill and Gifford. Although they have proved to be of great value for estimating diffusion of dilute, fully-developed and time-averaged plumes and puffs in the atmospheric boundary layer over relatively regular land, simple modifications do not appear to make them useful for other conditions. Thus, this class of models is of limited use at the outset. Perhaps, after more experience with actual accidental releases of heavy or light fluids from transport or storage containers, or from data gathered from planned experimental releases, a basis for modification of these simplistic conventional models may evolve.

Five more realistic basic models are suggested for consideration on an interim trial basis. They are shown schematically in Figure 49, and are called (1) gravity current, (2) free-jet with strong negative buoyancy, (3) impinging jet, (4) wall jet, and (5) wind-driven density mass. They are highly simplified, in effect ignoring that part of diffusion and transport in the atmosphere where concentrations of the contaminating substance remain very high. Thus, for example, plume-and-puff-like volumes may rise out of the edges of the high-concentration part of the original volume because of net local changes in density or wind shears. Any of the five basic models may be

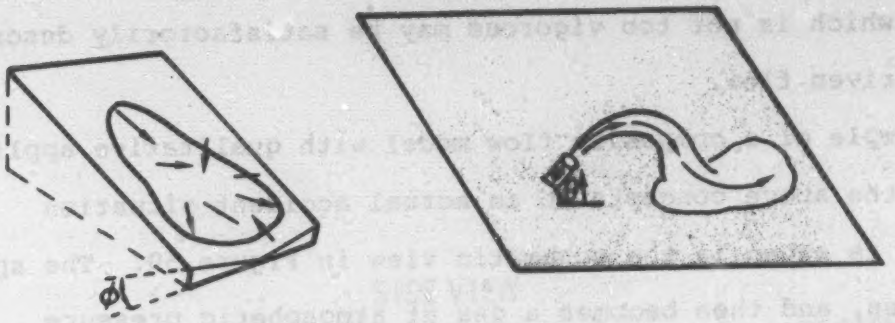

(1) THE GRAVITY CURRENT MODEL

(2) THE FREE, NEGATIVE-BUOYANCY JET MODEL

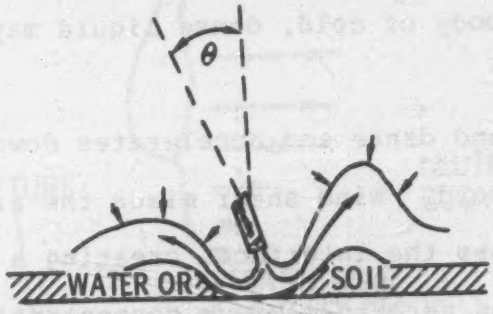

(3) THE IMPINGING-JET MODEL

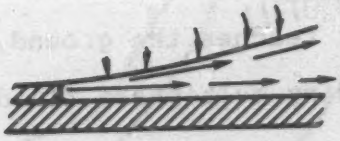

(4) THE WALL JET MODEL

(5) THE WIND-DRIVEN, DENSITY-MASS MODEL

Figure 49. Five basic models representing first approximations to Cl_2, NH_3, and CH_4 accidental release, transport and diffusion.

combined with any of the others to produce a reasonable first estimate of the most hazardous condition expected at a given site. For example, a wall jet which is not too vigorous may be satisfactorily described as a gravity-driven flow.

An example of a composite flow model with qualitative application of some of the above concepts to an actual accident situation description is shown in the schematic view in Figure 50. The spillage first flashes, and then becomes a gas at atmospheric pressure containing liquid droplets consisting of both the spilled substance and atmospheric water. A significant body of cold, dense liquid may also flow along the ground.

The multiphase fluid is cold and dense and accelerates downward and, as it reaches the ground, outward. Wind shear mixes the air and the intruding multiphase fluid across the interface, creating a transition zone of atmosphere having zero-to-maximum concentration values. Wind stress also moves and spreads the mass of contaminated air. However, these processes may not have had sufficient time to cause the contaminated mass to form into a simple, fully developed, or similarity condition flow. Additionally, heating from several sources or entrainment of less saturated air causes droplets to evaporate and density to reduce so that the negative buoyancy changes to neutral buoyancy or even to positive buoyancy. In each of the alternate buoyancy conditions it may be expected that important differences in the mean and turbulent flow regimes will exist within the contaminated gas volume. The mechanisms of mixing will differ somewhat and sinking and spreading flow may change to flow which lifts off the ground.

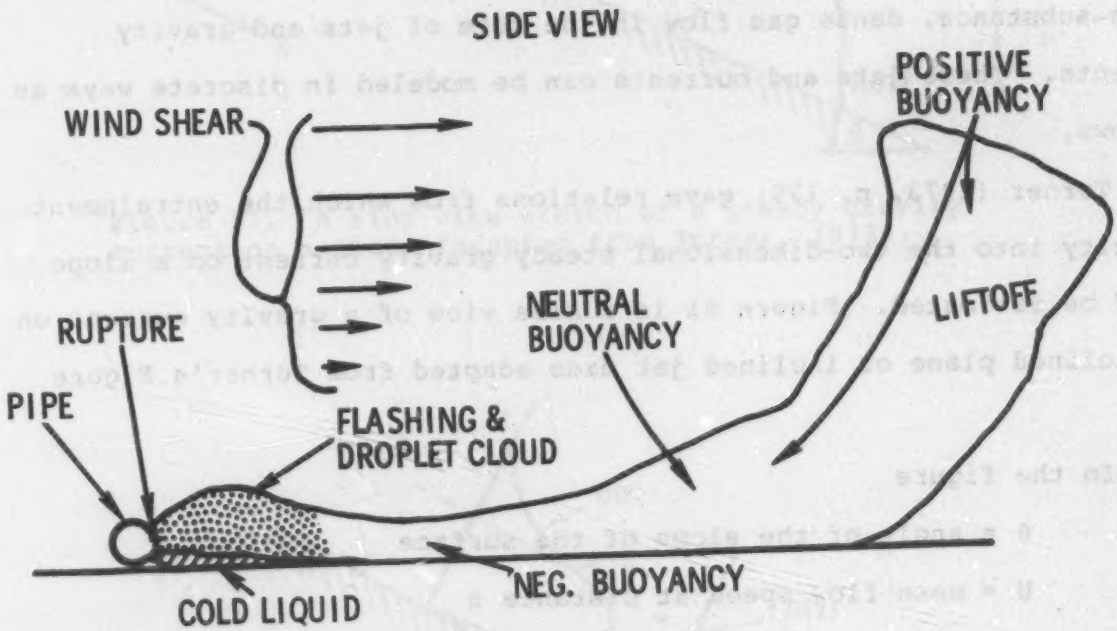

Figure 50. A schematic composite of a higher-order-approximation model of transport and diffusion in a hazardous gas accident.

These basic models do not account well for the effects of roughness and loose confinement. Finite difference solutions to the Navier-Stokes equations or fluid laboratory experiments may be required for these factors.

3.3 Jets and Gravity Currents

As noted above, a composite model would incorporate two-phase, three-substance, dense gas flow in the form of jets and gravity currents. These jets and currents can be modeled in discrete ways as follows.

Turner (1973, p. 179) gave relations from which the entrainment velocity into the two-dimensional steady gravity current on a slope could be estimated. Figure 51 is a side view of a gravity current on an inclined plane or inclined jet mass adapted from Turner's Figure 6.7.

In the figure

θ = angle of the slope of the surface

U = mean flow speed at distance x

h = average depth of the gravity current calculated as

$$h = U^{-1} \int_0^\infty u\,dz \quad \text{where } u = \text{speed at distance } x$$

g' = buoyancy force calculated as

$$g' = g\{(\rho_i - \rho_e)/\rho_e\}$$

By continuity, in a non-flowing, non-turbulent environment, the entrainment speed is

$$We = d(Uh)/dx \quad \text{or}$$

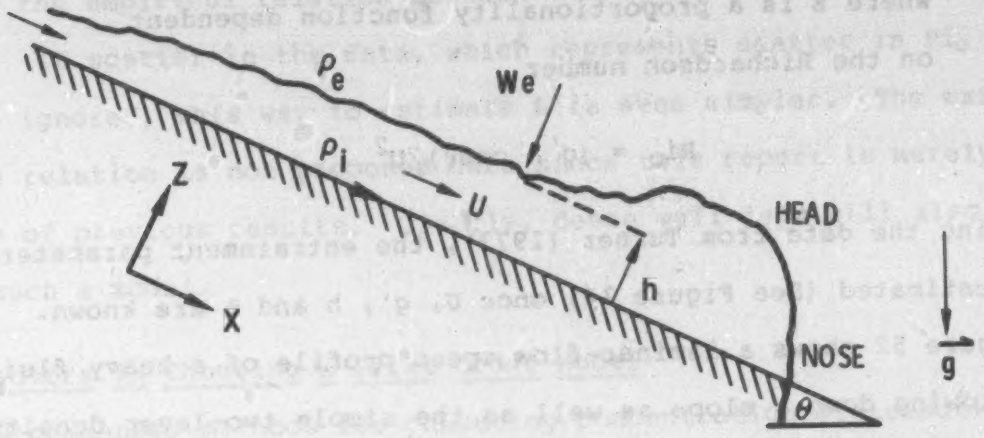

Figure 51. A side view sketch of a steady gravity current on a slope (adapted from Turner, 1973).

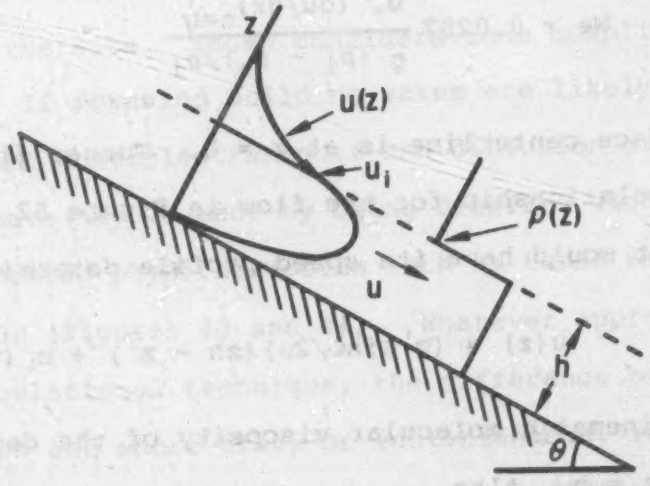

Figure 52. A speed profile for a heavy layer flowing laminarly down a smooth slope (adapted from Turner, 1973).

$$We = EU$$

where E is a proportionality function dependent on the Richardson number

$$Ri_o = (g' h \cos\theta)/U^2$$

Using the data from Turner (1973), the entrainment parameter, E, can be estimated (See Figure 14) once U, g', h and θ are known.

Figure 52 shows a laminar-flow speed profile of a heavy fluid layer flowing down a slope as well as the simple two-layer density profile.

Csanady (1978) provided an alternative method of estimating the entrainment speed at the density interface shown in Figure 52.

$$We = 0.0287 \frac{u_*^2 \, (du/dz)_{z=h}}{g \, (\rho_i - \rho_e)/\rho_i}$$

where the interface centerline is at z = h. Turner (1973) calculated the flow speed relationship for the flow in Figure 52 as an inclined plume; a wall jet would have its speed profile determined differently:

$$u(z) = (g' \sin\theta/2\nu)(zh - z^2) + u_i (z/h)$$

where ν is the kinematic molecular viscosity of the dense fluid and u is the speed at z = h. Also,

$$u_i/U = 2 - (Uh/6\nu)(Ri_o \tan\theta)$$

It would be possible to develop a mathematical model along lines

similar to those outlined above for a gravity current. Figure 15 showed the empirical relation between the entrainment parameter and the slope. If scatter in the data, which represents scatter in Ri_o values, can be ignored, this way to estimate E is even simpler. The exact form of the relation is not proposed here since this report is merely a survey of previous results. Clearly, dense wall jets will also fit into such a model.

3.4 Factors in Choosing a First Order Model

Recommended methods for computing concentration distribution for some of the five models are discussed in Section 4. The choice of first order flow model or combination of models to be used will depend upon the specific site topography, building arrangement, temperature, wind and turbulence intensity, and upon the details of gas transport and storage near the site. These considerations complicate specific model selection. If downwind building wakes are likely to interfere with application of a simple transport and diffusion concept, then a first order estimate may be made by using detailed wind tunnel observations of scaled physical models such as those reported by Yang and Meroney (1970) (Figures 43 and 44). Whatever approach is used for developing a calculational technique, the difference between time averaged variables and short time, or instantaneous, variables must be given constant consideration. Their values may differ by orders of magnitude.

Distance scales of transport may be categorized as follows:

(1) 1 to 30 km. Gaussian and fully developed mixing concepts may be useful.

(2) 0.5 to 2 km. Gaussian parameterizations of the diffusion equations may be useful; however, irregular and incomplete development of turbulent mixing and high density may cause erroneous transport and diffusion estimates.

(3) Less than 1 km. Special models will be required beyond those appropriate for (2) above, particularly when the distance from the released gas volume is less than about 10 volume diameters.

Roughness scale lengths and confinement lengths for several broad categories require attention:

(1) Open, nearly smooth terrain

(2) Coastal areas

(3) Continental river valley

(4) Complex terrain

(5) Built-up urban areas

The choice or rejection of basic models will depend on knowledge of individual local terrain features and of local meteorological phenomena. It will also depend on the location of the release in relation to the topography. For example, a gas release from a cliff top into the free air will require a different treatment of the same roughness feature than would an elevated release above the roughness feature, or than a release in the depression below the feature. A jet or plume model might fit the free fall from a cliff. A very complex flow might result from a somewhat lower release, where a gravity-current model might be more appropriate.

SECTION 4.0 Interim Methods for Estimating Concentration

4.1 Three Possible Methods

The composite flow model mentioned in Section 3.2 (Figure 50), if showing all possible major features, would contain boiling-liquid flow, two-phase, and three-substance dense gas flows as jets or gravity currents. This model would be the starting point for describing plume or puff flow which would be both irregular and not fully developed, but, in time, approaching near-neutral, fully developed conditions. The latter flows are amenable to description by the familiar empirical Gaussian models of plume expansion and concentration distribution. After reviewing and analyzing relevant observations and physical concepts of the hazards of accidental gas releases applicable to the problem of reactor support facility vulnerability, the following conclusion was reached: Gas volumes which can be sufficiently well modeled by the Gaussian techniques would have to be so dilute (density within a few percent of ambient) that these techniques would not be relevant except for the low concentration problems of gas ignition, toxicity and corrosiveness. Even then, based on the few available observations, most gas clouds which undergo ignition appear to do so well before they can develop into Gaussian-theory applicability.

The interim methods of estimating concentration fields of a relatively large (many cubic meters) release of hazardous gas may follow one or more of the following basic techniques:

(1) Modified Gaussian plume or puff models

(2) Relatively simple gravity current or jet models

(3) Numerical solution of coupled equations of motion,

with interim parameterizations of turbulent transfer of heat, chemical species, mass and momentum

The most simple, physically acceptable, and quickest method to apply is based on technique (2). Only a small amount of development appears to be required to make existing research results from such models applicable to the specific problem at hand. Technique (1) relates to models which are frequently not correct for the present problem in either physical principle or in result. Technique (3) has the most promise of providing physically realistic estimates of concentration distribution as a function of time and space. This technique is discussed later in Section 4.4.

4.2 A Modified Gaussian Plume-Puff Model

The Vulnerability Model prepared for the U. S. Coast Guard (Eisenberg, 1975) uses an air dispersion submodel which is a typical Gaussian plume for moderate rate, continuous releases. If the spill is liquid and rapid, and rapidly vaporizes, the model calls for a puff modified to include a hemispheric core of pure vapor surrounded by a region where the concentration decreases according to the Gaussian technique (See pages 33 to 48 of Eisenberg, 1975). While plume meander is considered, peak concentration estimation methods are not used, and buoyancy effects are not incorporated. Wing (1976) has discussed in detail relevant applications of Gaussian schemes. It is concluded that the air dispersion submodel of the Vulnerability Model sometimes may be adequate for use if proper care is taken to evaluate its applicability.

4.3 Simple Gravity Current or Jet Model

Based upon concepts of gravity driven slope flows discussed in section 3.3, it would be possible to derive a time history of intruding heavy gasses which would allow concentration estimates to be made. These would follow from considerations of entrainment-caused dilution and plume expansion.

Simpler techniques in this category would include scaling from either field release experiments or laboratory wind tunnel model experiments. An example of application for regulatory use in postulated accident scenario evaluation might be that of estimating intruding dense gas concentration at a building ventilation port. If the terrain is smooth and non-sloping, the empirical plots from Gideon and Putnam (1976) (Figures 5 and 6) may be used to estimate maximum ground-level concentration as a function of distance. For puff-like releases, the empirical data and formula developed by Van Ulden (1974) may be useful in estimating vertical and horizontal spread of the gas (Figures 11, 12, and 13).

The free, heavy jet or plume develops a cross-section concentration profile which is best estimated from empirical data such as those presented by Hoot, Meroney and Peterka (1973) in Figure 53. The figure shows normalized concentration, or

$$(XUD_o^2 / Q) \times 10^4$$

where D_o is initial plume diameter, U is crosswind averaged velocity (laminar flow), Q is source emission rate, and X is concentration.

Figure 54, from the same report, provides a basis for estimating maximum concentration in the plume as a function of longitudinal

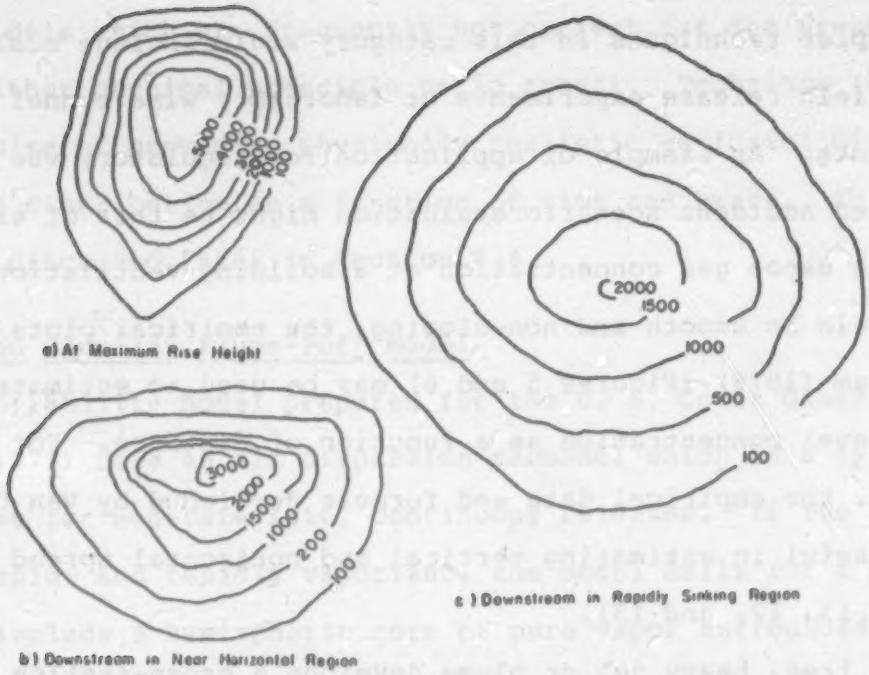

Figure 53. Cross section plots of concentration of heavy gas plume, $(XUD_o^2/Q) \times 10^4$ (from Hoot et al, 1973).

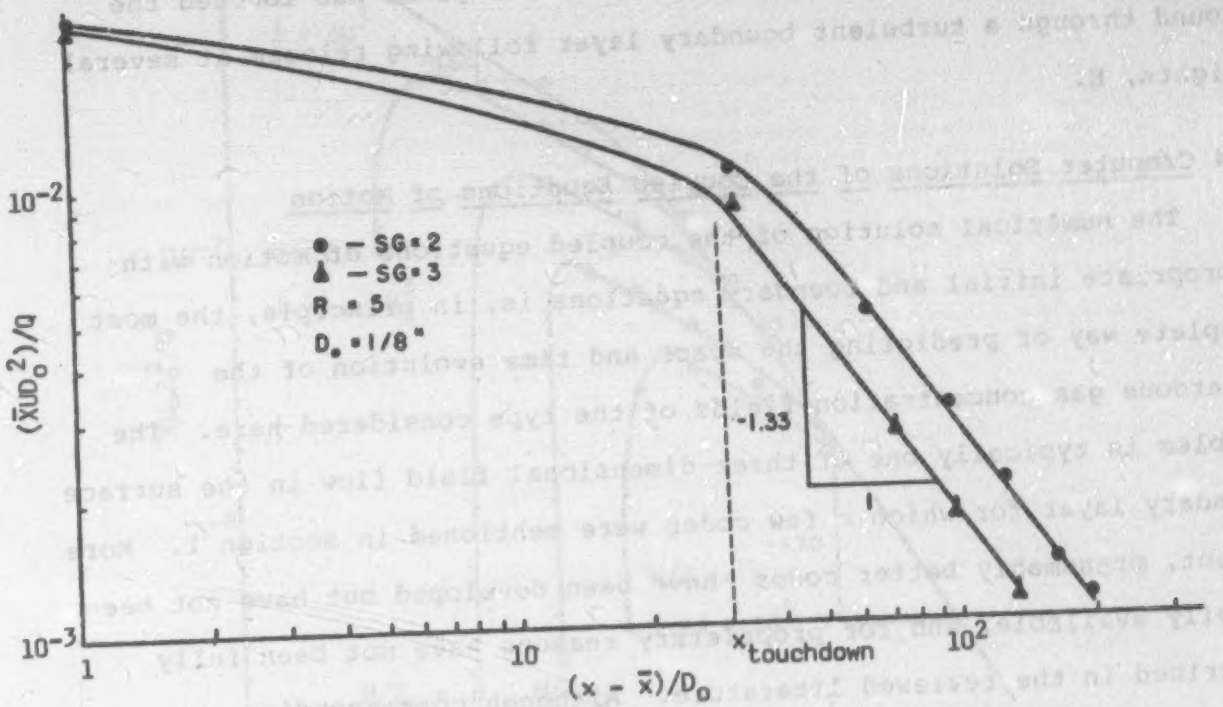

Figure 54. Maximum concentration vs downstream distance of plumes in a laminar crosswind, R = 5, D_o = 1/8 inch, x = horizontal distance to plume high point (adapted from Hoot et al, 1973).

distance before, during and after touchdown in a laminar wind. After touchdown the horizontal crossflow concentration profile is relatively uniform or flat. Figure 55 provides a similar basis for evaluation of concentration maxima at the surface after the plume has touched the ground through a turbulent boundary layer following release at several heights, H.

4.4 Computer Solutions of the Coupled Equations of Motion

The numerical solution of the coupled equations of motion with appropriate initial and boundary equations is, in principle, the most complete way of predicting the space and time evolution of the hazardous gas concentration fields of the type considered here. The problem is typically one of three-dimensional fluid flow in the surface boundary layer for which a few codes were mentioned in Section 1. More recent, presumably better codes have been developed but have not been readily available, and for proprietary reasons have not been fully described in the reviewed literature. Although corresponding two-dimensional model codes exist, they may not adequately represent some classes of transport and diffusion, but they are faster and less costly to run.

Several currently used models fall into the following categories: (1) marker and cell solutions (Hirt et al, 1975), (2) mixing coefficient and deformation modeling of turbulent stresses (Crawford, 1977; Spalding, 1972) and (3) second order parameterization schemes (Lewellen and Teske, 1975). Capabilities of these models are quite broad and could accommodate buoyant gas applications.

Figure 56 is a plot of wind vectors in a plane cutting vertically across a ditch or recessed highway that has a crossflow of air above

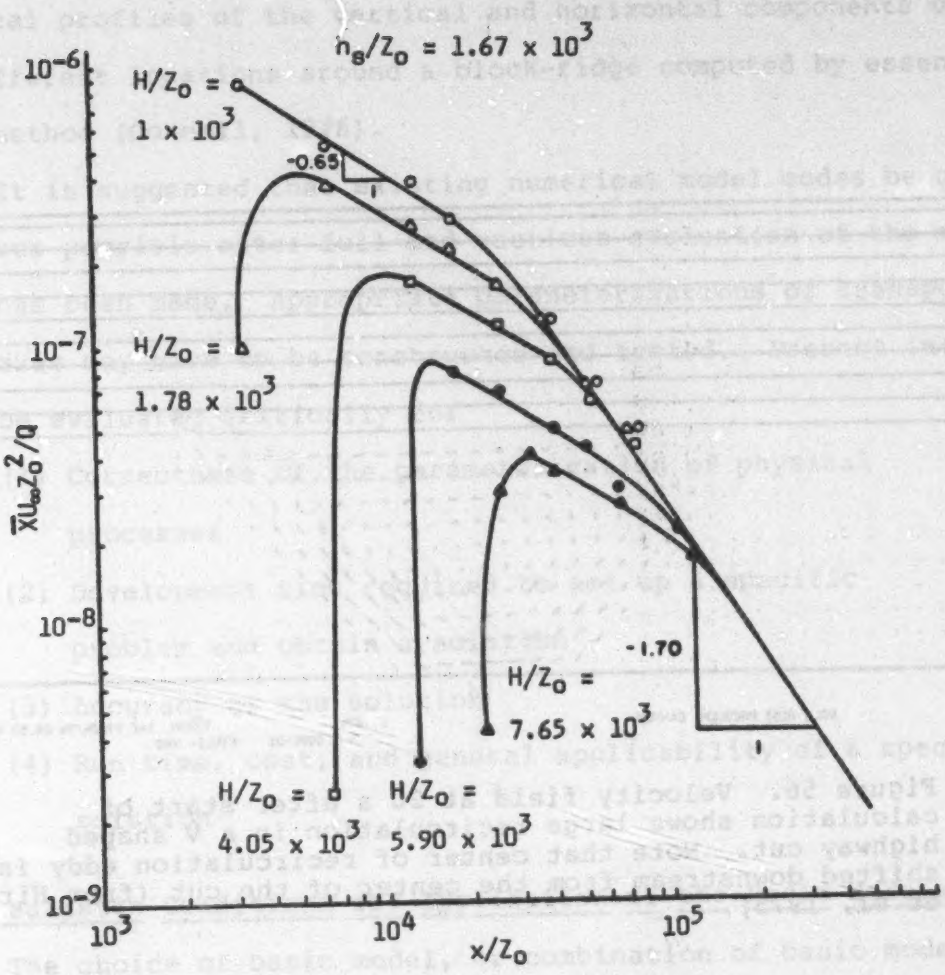

Figure 55. Non-dimensional, normalized plot for various release heights showing decay of plume maximum concentration downstream from touchdown point in turbulent boundary layer. h = stack height, H = plume height, Z_o = roughness length U_∞ = free stream velocity, Q = emission rate, x = distance downstream, and X = concentration (adapted from Hoot et al, 1973).

READEX FICHE

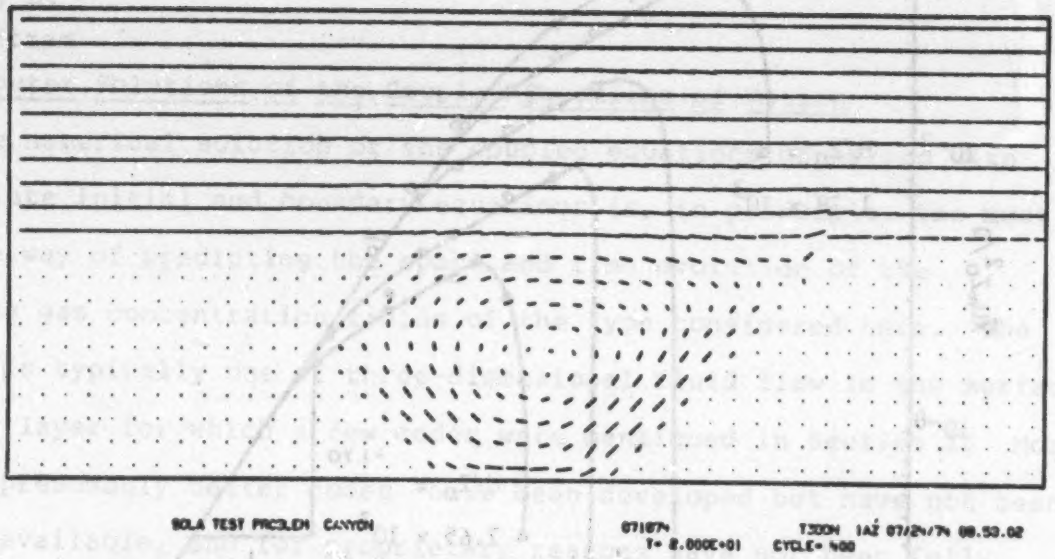

Figure 56. Velocity field at 20 s after start of calculation shows large recirculation in a V shaped highway cut. Note that center of recirculation eddy is shifted downstream from the center of the cut (from Hirt et al, 1975).

it. These vectors were derived using the two-dimensional program (called SOLA) described by Hirt et al (1975). Figure 57 contains vertical profiles of the vertical and horizontal components of the wind at different locations around a block-ridge computed by essentially the same method (Connell, 1976).

It is suggested that existing numerical model codes be used wherever possible after full and cautious evaluation of the merit of each has been made. Appropriate parameterizations of transport processes may have to be constructed and tested. Present interim codes must be evaluated critically for

(1) Correctness of the parameterization of physical processes

(2) Development time required to set up a specific problem and obtain a solution

(3) Accuracy of the solution

(4) Run time, cost, and general applicability of a specific solution

4.5 Realistic Conditions for Application of the Basic Models

The choice of basic model, or combination of basic models, is very much determined by the nature of the terrain, building geometry, the types, times and probabilities of local meteorological features, and the exact conditions of storage, transport and release of potentially hazardous gases. Transport and diffusion processes will be strongly influenced by the time scales and the length scales inherent in each specific physical situation. These detailed aspects of the hazardous gas problem are beyond the scope of this report.

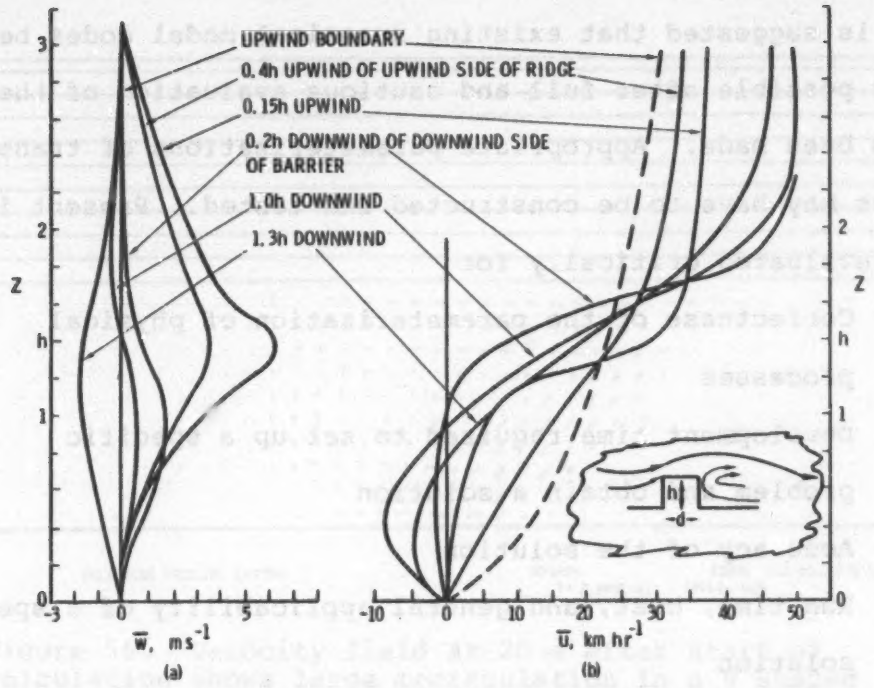

Figure 57. Vertical profiles of (a) vertical wind speed and (b) horizontal wind speed upwind and downwind of a 2-d ridge computed by a simplified marker and cell technique (from Connell, 1976).

SECTION 5. Recommendations for Needed Research and Development

Field measurements are needed to properly test interim models of transport and diffusion of hazardous gases as they might affect operating facilities of a nuclear power plant. This literature search did not identify a single set of experiments which are entirely suitable as a field study of a realistic spill. Van Ulden's 1974 studies are of a type that come closest.

For a variety of practical reasons, it is considered best to attack the problem simultaneously from three different approaches:

(1) Field studies on several size scales

(2) Wind-tunnel and water-channel simulations

(3) Mathematical simulations

However, emphasis should be placed on obtaining adequate observations from several realistic yet simple full- or near-full-scale atmospheric concentration experiments. The next step is to test mathematical simulations against adequate observations by using the most promising models.

Briggs (1975) has listed several topics which need further study. The following have been taken from his list:

(1) Diffusion of a horizontal jet, considering its attachment and tendency to act as a wall jet, as well as liftoff of positively buoyant flow or settling of negatively buoyant flow

(2) Positively buoyant masses attached to the ground, such as point jets, building cavities, and line sources

(3) Flow behavior of dense gas over a rough surface

(4) Transport and diffusion of dense gas as a function of each of the following properties:

- source strength
- nature of underlying surface
- ambient turbulence
- stratification
- wind shears relative to frontal velocity of a dense gas

(5) Amount of initial dilution, shape and momentum of the initial gas region

(6) Conditions in the atmosphere and degree of dilution at which the dense gas behaves like ambient air

In addition, the mechanisms of the following processes will have to be studied:

(1) Front or nose mixing

(2) Top and side mixing (not necessarily the same mechanism)

(3) Droplet-gas cloud (two phase, four substance) processes and change of phase and density

(4) Gas concentration layering

(5) Transition to different mixing and dilution rate regimes

(6) Crosswind effects above a stream, open or channeled, dense gas

The mathematics, approximations, or parameterizations of these processes must be developed so that actual phenomena in the flows listed above can be properly represented.

The Department of Energy has proposed a major research program to

study transport and diffusion of pressurized and cryogenic liquified fuels released to the atmosphere (U.S. Department of Energy, 1978). Utilizing this program to help meet the requirements discussed here seems to be expedient. However, the range of conditions, processes and gases to be studied by DOE would appear to leave much of interest to NRC to be learned by a separately designed and sponsored program of study.

SECTION 6. Conclusions

One objective of this report was to evaluate the literature as a guide for modeling transport and diffusion of hazardous gases. It has become clear that few previous efforts have researched those factors that could lead to detailed and quantitative knowledge of the fluid physics of hazardous, high concentration, non-ambient density gas releases into the atmosphere near the ground. A program should be initiated for the development of economical and effective analytical and predictive tools for this type of hazard assessment.

The conclusion is also reached that "plume" or "puff" models may not be suited for use in interim concentration estimates, although near-field, grossly conservative factors can be derived from conventional Gaussian approaches. Five alternative physical models were suggested.

Better models could come from a two- or three-dimensional iterative solution to the coupled equations of motion.

Any effort to validate current models must depend upon field measurement studies. A planned balance of fluid-laboratory study, mathematical simulation and field measurement by knowledgeable groups is recommended in order to provide a dependable set of evaluative tools for regulatory purposes.

References

Abbey, R. F., Jr., 1976: Concentration measurements downwind of buildings - previous and current experiments. Preprints - Third symposium on Atmospheric Turbulence, Diffusion, and air quality (Raleigh, NC), Am. Meteor. Soc., Boston, 247-254.

Barr, S., R. E. Luna, W. E. Clements, and H. W. Church, eds., 1977: Workshop on Research Needs for Atmospheric Transport and Diffusion in Complex Terrain. CONF-7609160,ERDA/DBER, Washington, DC, 20545.

Barry, P. J., 1964: Estimation of downwind concentration of airborne effluents discharged in the neighborhood of buildings. AECL-2043, Atomic Energy of Canada, Ltd, Chalk River.

Briggs, G. A., 1975: Research required for predicting behavior of pressurized gases escaping into the atmosphere. Internal NOAA/ATDL Report 75/5.

Connell, J. R., (unpublished, 1976): Numerical fluid mechanical simulation of mean wind velocities influenced by an isolated ridge. University of Tenn. Space Inst.

Carpenter et al, 1978: Liquified natural gas wind tunnnel simulation and instrumentation assessments. DOE contract report SAN/W1364-01, by R & D Assoc. and Colorado State Univ., Wash., DC.

Crawford, T. L., 1977: Numerical modeling of complex two and three dimensional flow and diffusion problems in the natural air environment. Thesis, Univ. of Waterloo, Ontario.

Csanady, G. T., 1978: Turbulent interface layers. J. of Geoph. Res., 83, 2329-2342.

Dickson, C. R., G. E. Start and E. H. Markee, Jr., 1969: Aerodynamic effects of the EBR-II reactor complex on effluent concentration. Nuclear Safety, 10, 228-242.

Eisenberg, N. A., C. J. Lynch and R. J. Breeding, 1975: Vulnerability model - a simulation system for assessing damage resulting from marine spills. Contract Rpt., Enviro Control, Inc., CG-D-137-75 (From NTIS as AD-A015 245), 333 pp.

Gideon, D. N., and A. A. Putnam, 1977: Dispersion hazards from spills of LNG on land and on water. Cryogenics, 17, 9-15.

Gifford, F. A., 1960: Peak to average concentration ratios according to a fluctuating plume disperson model. Int. J. Air Pollut., 3, 253-260.

Gifford, F. A., 1976: Turbulent diffussion - typing schemes: A review. Nuclear Safety, 17, 68-86.

Halitsky, J., 1968: Gas diffusion near buildings. In Meteorology and Atomic Energy 1968. (D. H. Slade, ed), USAEC, NTIS TID-24190, 221-255.

Halitsky, J., and K. Woodward, 1974: Atmospheric diffusion experiments at a nuclear plant site under light wind inverison conditions. Proceedings of symposium on atmospheric diffusion and air pollution (Santa Barbara), Amer. Meteor. Soc., Boston.

Hansen, A. C., J. A. Peterka and J. E. Cermak, 1974: Wind-tunnel measurements in the wake of a simple structure in a simulated atmospheric flow. Contract Rpt. NASA CR-2540, Colo. St. Univ., Ft. Collins, 39 pp.

Hardee, H. C.,Jr., and D. O. Lee, 1975: Expansions of clouds from pressurized liquids. Accid. Anal. and Prev., 7, 91-102.

Hinds, W. T., 1969: Peak-to-mean concentration ratio from ground-level sources in building wakes. Atmos. Env., 3, 145-156.

Hirt, C. W., B. D. Nichols and N. C. Romero, 1975: SOLA - A numerical solution algorithm for transient fluid flows. Los Alamos Sci. Lab., Rpt. LA-5852, Univ. of Calif.

Hoot, T. G., R. N. Meroney and J. A. Peterka, 1973: Wind tunnel tests of negatively buoyant plumes. Grant report: CER 73-74TGH-RNM-JAP-13, Colorado State Univ., Ft. Collins.

Lewellen, W. S., and M. E. Teske, 1975: Turbulence modeling and its application to atmospheric diffusion. EPA-600/4-75-016, ARAP, Inc., Princeton.

Luna, R. E., and H. W. Church, 1972: A comparison of turbulence intensity and stability ratio measurements to Pasquill stability classes. J. Appl. Meteor., 11, 663-669.

Meroney, R. N., and B. T. Yang, 1971: Wind-tunnel studies of gaseous mixing due to various stack heights and injection rates above an isolated structure. Contract Rpt. CER 71-72RNM-BTY 16, Colo State Univ., Ft. Collins.

Neff, D. E., R. N. Meroney and J. E. Cermak, 1976: Wind tunnel study of the negatively buoyant plume due to an LNG spill. Contract report: CER 76-77-DEN-RNM-JEC 22, Colorado State Univ., Ft. Collins.

Pasquill, F., 1974: Atmospheric Diffusion, 2nd ed., John Wiley & Sons, Inc., 429 pp.

Raynor, G. S., P. Michael, R. M. Brown and S. Sethu Raman, 1975: Studies of Atmospheric diffusions from a nearshore oceanic site. J. Appl. Meteor., 14, 1080-1094.

Slade, D. H., 1962: Atmospheric diffusion over Chesapeake Bay. Mon. Wea. Rev., 90, 217-224.

Spalding, D. B., 1972: A novel finite difference formulation for differential expressions involving both first and second derivatives. Int. Journal of Numerical Meth. in Engrg., 4, 551-559.

Start, G. E., J. H. Cote, C. R. Dickson, N. R. Ricks, G. R. Ackermann, J. F. Sogendorf, 1977: Rancho Seco building wake effects on atmospheric diffusion. Air Resources Labs, Idaho Falls, NOAA Tech. Mem. ERL ARL-69, 185 pp.

Symes, C. R., and R. N. Meroney, 1970: Cone frustums in a shear layer. Contract Rpt. CER 70-71CRS-RNM11, Colo State Univ., Ft. Collins.

Turner, J. S., 1973: Buoyancy Effects in Fluids, Cambridge University Press, 367 pp.

Turner, J. S., 1978: Double-diffusive intrusions into a density gradient. J. of Geoph. Res., 83, 2887-2901.

U. S. Department of Energy, 1978: An Approach to Liquified Natural Gas (LNG) Safety and Environmental Control Research. U. S. Department of Energy Rept. DOE/EV-0002.

U. S. Nuclear Regulatory Commission, 1972: Onsite meteorological programs. Regulatory Guide 1.23, USNRC, Washington, DC.

Van der Hoven, I., 1976: A survey of field measurement of atmospheric diffusion under low-wind-speed inversion conditions. Nucl. Safety, 17, 223-230.

Van Dolah, R. W., 1963: Fire hazards of cryogenic fuels. Symposium on cryogenic storage and handling of hydrogen and natural gas. (Portland, OR), Society of Fire Protection Engineers, Boston, MA.

Van Ulden, A. P., 1974: On the spreading of a heavy gas released near the ground. Proceedings - Loss prevention and safety promotion in the process industries, Switzerland, May, C. H. Buschmann (ed) Elsevier Scientific Publishing Co., The Hague.

Wing, J., 1976: Toxic vapor concentration in the control room of a nuclear power plant following a postulated accidental release. Draft NRC report, Accident Analysis Branch, USNRC, Washington, DC.

Yang, B. T., and R. N. Meroney, 1970: Gaseous dispersion into stratified building wakes. Contract report to USAEC, COO-2053-3, Colo State Univ., Ft. Collins.

DISTRIBUTION:

U. S. Nuclear Regulatory
Commission (145 copies for RE)
Division of Document Control
Distribution Services Branch
7920 Norfolk Branch
Bethesda, MD 20014

U. S. Nuclear Regulatory
Commission (5)
Hydrology Meteorology Branch
Washington, DC 20555
Attn: E. H. Markee, Jr.

U. S. Department of Energy
Division of Environmental
Control Technology
Washington, DC 20545
Attn: J. Cece

U. S. Department of Energy
Division of Health and
Environmental Research
Washington, DC 20545
Attn: F. Hudson
D. S. Ballantine

Battelle Pacific Northwest
Laboratories (10)
Richland, WA 99352
Attn: J. R. Connell

U. S. Nuclear Regulatory
Commission
Site Safety Research Branch
Washington, DC 20555
Attn: R. F. Abbey, JR.

NOAA/ATDL
Oak Ridge, TN 37830
Attn: F. A. Gifford
G. A. Briggs

NOAA/ERL/ARL
Silver Spring, MD 20910
Attn: I. Van der Hoven
G. E. Start

Colorado State University
Ft. Collins, CO 80521
Attn: R. N. Meroney

Los Alamos Scientific Laboratory
Los Alamos, NM 87544
Attn: C. W. Hirt

Virginia Polytechnic & State
University
Blacksburg, VA 24060
Attn: R. E. Akins

U. K. Atomic Energy Authority
Wigshaw Lane, Culcheth Warrington
England, WA3 4 NE
Attn: G. D. Kaiser

Brookhaven National Laboratory
Upton, NY 11973
Attn: R. E. Meyers

Argonne National Laboratory
Argonne, IL 60439
Attn: B. B. Hicks

1233 J. M. Taylor
1711 M. R. Madsen
3312 R. B. Stump
4410 D. J. McCloskey
4413 D. C. Aldrich
4414 D. E. Bennett
4443 A. R. Ducharme, Jr.
4514 E. L. Wilmont
4530 R. W. Lynch
4533 B. D. Zak
4533 H. W. Church (5)
4533 F. M. Gelbard
4723 D. O. Lee
5512 H. C. Hardee, Jr.
8266 E. A. Aas
3141 T. L. Werner (5)
3151 W. L. Garner (3)
for DOE/TIC (Unlimited
Release)
3154-3 R. P. Campbell (25)
(for NRC distribution
to NTIS)

NRC FORM 335 (7-77) U.S. NUCLEAR REGULATORY COMMISSION

BIBLIOGRAPHIC DATA SHEET

1. REPORT NUMBER (Assigned by DDC): NUREG/CR-1152

4. TITLE AND SUBTITLE (Add Volume No., if appropriate): Recommended Methods for Estimating Atmospheric Concentrations of Hazardous Vapors After Accidental Release Near Nuclear Reactor Sites

2. (Leave blank)

3. RECIPIENT'S ACCESSION NO.

7. AUTHOR(S): J. R. Connell and H. W. Church

5. DATE REPORT COMPLETED: MONTH October, YEAR 1979

9. PERFORMING ORGANIZATION NAME AND MAILING ADDRESS (Include Zip Code)

Environmental Research Division
Sandia Laboratories
Albuquerque, N.M. 87185

DATE REPORT ISSUED: MONTH April, YEAR 1980

6. (Leave blank)

8. (Leave blank)

12. SPONSORING ORGANIZATION NAME AND MAILING ADDRESS (Include Zip Code)

Hydrology-Meteorology Branch
Division of Site Safety and Environmental Analysis
Office of Nuclear Reactor Regulation
U.S. Nuclear Regulatory Commission
Washington, D. C. 20555

10. PROJECT/TASK/WORK UNIT NO.: FIN A1110

11. CONTRACT NO.

13. TYPE OF REPORT: Topical Report

PERIOD COVERED (Inclusive dates)

15. SUPPLEMENTARY NOTES

14. (Leave blank)

16. ABSTRACT (200 words or less)

A literature survey was done which addresses the problems of atmospheric transport and diffusion of positively and negatively buoyant hazardous gases. Typical hazardous vapors of concern are chlorine, ammonia, and vapors from liquified natural gas. The objective was to determine the state of the art for analyzing hazards to nuclear power plants. It was found that existing computer simulations, and fluid laboratory and field measurements provide a basis from which to analyze the problem, but are insufficient for the establishment of firm hazards criteria. Within this report, existing models with predictive capability have been categorized, and available measurements of transport, diffusion and gas concentration have been organized by flow condition type in order to assess model accuracy. Operational models have not been found which are entirely suitable for NRC Regulatory predictive purposes. However, suggestions are made for model selection. Recommendations are also given for further research in areas where such efforts should prove profitable. It is concluded that the need is great for field scale measurements for model development and testing.

17. KEY WORDS AND DOCUMENT ANALYSIS

17a. DESCRIPTORS

17b. IDENTIFIERS/OPEN-ENDED TERMS

18. AVAILABILITY STATEMENT: Unlimited

19. SECURITY CLASS (This report): Unclassified

21. NO. OF PAGES

20. SECURITY CLASS (This page)

22. PRICE $

*U.S. GOVERNMENT PRINTING OFFICE : 1980 0-620-268/117

UNITED STATES
NUCLEAR REGULATORY COMMISSION
WASHINGTON, D. C. 20555

OFFICIAL BUSINESS
PENALTY FOR PRIVATE USE, $300

POSTAGE AND FEES PAID
U.S. NUCLEAR REGULATORY
COMMISSION

U.S. MAIL